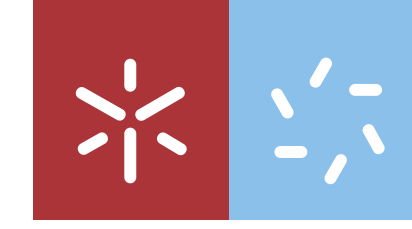**Universidade do Minho**
Escola de Ciências

Ana Teresa Moutinho Barbosa

Anti-*RAS1* and anti-*RIM101* oligomers for controlling *Candida albicans* filamentation under different body fluids

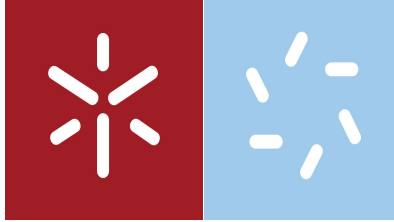janeiro de 2021

Universidade do Minho
Escola de Ciências

Ana Teresa Moutinho Barbosa

Anti-*RAS1* and anti-*RIM101* oligomers for controlling *Candida albicans* filamentation under different body fluids

Dissertação de Mestrado
Mestrado em Genética Molecular

Trabalho efetuado sob a orientação da
Doutora Sónia Carina Morais da Silva e da **Professora Doutora Ana Paula Fernandes Monteiro Sampaio Carvalho**

janeiro de 2021

DIREITOS DE AUTOR E CONDIÇÕES DE UTILIZAÇÃO DO TRABALHO POR TERCEIROS

Este é um trabalho académico que pode ser utilizado por terceiros desde que respeitadas as regras e boas práticas internacionalmente aceites, no que concerne aos direitos de autor e direitos conexos.

Assim, o presente trabalho pode ser utilizado nos termos previstos na licença abaixo indicada.

Caso o utilizador necessite de permissão para poder fazer um uso do trabalho em condições não previstas no licenciamento indicado, deverá contactar o autor, através do RepositóriUM da Universidade do Minho.

Acknowledgements /Agradecimento

"Somewhere, something incredible is waiting to be known." - Carl Sagan

Aos meus pais agradeço todo o apoio e carinho!

Às minhas irmãs, agradeço todo o amor e apoio incondicional!

Ao Hugo, agradeço todo amor e carinho, assim como, o apoio constante, compreensão e por sempre acreditar em mim!

~

STATEMENT OF INTEGRITY

I hereby declare having conducted this academic work with integrity. I confirm that I have not used plagiarism or any form of undue use of information or falsification of results along the process leading to its elaboration.

I further declare that I have fully acknowledged the Code of Ethical Conduct of the University of Minho.

Sumário

Candida albicans continua a ser a espécie do género *Candida* responsável por maior número de infeções fúngicas em humanos. A patogenicidade de *C. albicans* está relacionada com a capacidade de transitar da forma de levedura para a forma filamentosa (dimorfismo). Esta transição de forma tem sido relacionada com alguns genes, entre eles *RAS1* e *RIM101*. Assim, o principal objetivo deste trabalho, com base na terapia antisense (TA), foi desenvolver oligómeros antisense (OAS) capazes de reduzir a expressão genética dos genes *RAS1* e *RIM101*. Pretende-se assim contribuir para o desenvolvimento de um cocktail de OAS capazes de controlar a filamentação de *C. albicans* em diferentes fluidos corporais humanos.

Assim, como primeira tarefa avaliou-se a capacidade de filamentação de *C. albicans* em fluidos corporais humanos simulados, preparados a diferentes pH. Verificou-se que *C. albicans* é capaz de filamentar em saliva e urina artificial com diferentes valores de pH (4, 5.8 e 7), evidenciando a elevada capacidade de adaptabilidade e plasticidade de *C. albicans* em diferentes contextos ambientais.

A segunda tarefa consistiu no desenho de dois OAS, o anti-*RAS1* e o anti-*RIM101*, e na validação da sua funcionalidade in vitro. A ausência de citotoxidade de anti-*RAS1* 2'-*O*MethylRNA (2'OMe) e anti-*RIM101* 2'OMe, conjuntamente com a capacidade de reduzir a níveis significativos tanto a expressão dos genes *RAS1* e *RIM101*, como a filamentação de *C. albicans* em diferentes fluidos corporais simulados, valida a aplicabilidade da TA no controlo da virulência de *C. albicans*.

Assim, este trabalho reforça a possibilidade do desenvolvimento de novos antifúngicos a partir de um cocktail de OAS para o tratamento de candidíases.

Palavra-chave: Candidíases, formas filamentosas, mímicos de ácidos nucleicos, modificação 2'-*O*MethylRNA

Abstract

Candida albicans remains the species of the genus *Candida* responsible for the largest number of fungal infections in humans. The pathogenicity of *C. albicans* is related with the ability to switch from yeast to filamentous forms (dimorphism). *RAS1* and *RIM101* genes are identified as important regulators of this phenomenon. Thus, based on antisense therapy (AST), the main goal of this work was to develop antisense oligomers (ASOs) capable of reducing the genetic expression of the *RAS1* and *RIM101* genes. It is intended to contribute to the development of an ASOs cocktail capable of controlling the filamentation of *C. albicans* in different human body fluids.

So, as a first task, the filamentation capacity of *C. albicans* on human body fluids simulated at different pH was evaluated. It was verified that *C. albicans* is able to develop filaments on saliva and artificial urine under different pH values (4, 5.8 and 7), demonstrating the high plasticity and adaptability of *C. albicans* on different environmental contexts.

The second task was to design two ASOs, anti-*RAS1* and anti-*RIM101*, and to validate its functionality *in vitro*. The absence of anti-*RAS1* 2'-*O*MethylRNA (2'OMe) e anti-*RIM101* 2'OMe cytotoxicity, jointly with its ability to reduce the expression of *RAS1* and *RIM101* genes and *C. albicans* filamentation on different simulated body fluids to significant levels, validates the applicability of AT to control of *C. albicans* virulence.

Thus, this work reinforces the possibility of developing new antifungals from an ASO cocktail to be used in the treatment of candidiasis.

Keywords: Candidiasis, filamentous forms, mimics of nucleic acids, 2'-*O*MethylRNA modification

Table of contents

List of Abbreviations and Symbols

AST- Antisense Therapy

ASO- Antisense Oligomers

cDNA- complementary DNA

CFUs- colony forming units

CHROMagarTM – Chromogenic Media Agar

D-MEM- Dulbecco's Modified Eagle's Medium

DNase I - Deoxyrybonuclease I

LIP- lipases

LNA- Locked nucleic acid

miRNAs- microRNAs

MOE- 2'-O-methoxyethyl

NTS- nucleotides

PBS- phosphate-buffered saline

PL- phospholipases

PMO- Phosphoroamidate morpholino oligomer

PNA- Peptide nucleic acid

PS- Phosphorothioate

RPMI- Roswell Park Memorial Institute

SAPs- secreted aspartyl proteinases

SDA- sabouraud dextrose agar

SDB- sabouraud dextrose broth

qRT-PCR- Quantitative Reverse transcription polymerase chain reaction

Tm- melting temperature

log CFU cm^{-2}- logarithm of the number of colony formation per square centimetre

List of Figures

24 h **(B)** of *C. albicans* cells grown on artificial urine (AU) pH 5.8 and artificial saliva (AS) pH 7. Error bars represent standard derivation. *Significant differences between single anti-*RAS1* 2'OMe and combined effect for the same time of incubation. +Significant differences between single anti-*RIM101* 2'OMe and combined effect for the same time of incubation (P <0.05). 46

List of Tables

Scope of the Thesis

Antisense oligomers (ASOs) and their analogues have been successfully utilized to silence gene expression for the treatment of many human diseases, however for controlling yeast's virulence determinants it was little exploited. *Candida albicans* filamentation is an important virulence factor regulated by set of genes, as is the case of the *RAS1* gene (involved on MAP kinase and cAMP/PKA cascades) and the *RIM101* gene (described as a pH signalling gene). In this sense, based on antisense therapy (AST), it is expected to develop ASOs capable of hybridizing with *RAS1* and *RIM101* mRNA, blocking its translation into the correspondent proteins. It is intended to contribute for creating a cocktail of therapeutic ASOs with capacity to control the filamentation of *C. albicans* on different human body fluids.

This thesis is divided into four chapters: the literature review (Chapter 1), the study of *C. albicans* behaviour on simulated human body fluids under different pH (Chapter 2) and the application of 2'-*O*MethylRNA antisense oligomers to control *RAS1* and *RIM101* virulence determinants and *Candida albicans* filamentation under different body fluids (Chapter 3). Chapter 1 is a literature review presenting the current knowledge of the biology, virulence factors and molecular pathways of *Candida albicans*. Moreover, an overview about antisense technology as a future strategy to control yeast virulence determinants as consequently *Candida* virulence factors, was performed. *Candida albicans* is characterized by its high success as a pathogenic agent, presenting high plasticity and adaptability to the environment. Thus, the second chapter aimed to study the behaviour of *C. albicans* on two simulated human body fluids (artificial saliva and urine) adjusted to different pH (pH 4, 5.8 and 7). As *Candida* infections have been associated with high morbidity and mortality, which is a public health problem, it is essential to develop new strategies. Antisense therapy has been utilized an alternative therapy in cancer and neurodegenerative diseases, in the recent decades. This approach is based on the use of a single sequence of antisense oligonucleotides that hybridizes with the target mRNA resulting in an inhibition of gene expression. Thus, the main goal of third chapter was to design and synthesis ASOs targeting the *RAS1* and *RIM101* mRNA and to validate, *in vitro*, its applicability. The fourth chapter summarizes the major conclusions reached during this work and future perspectives with this research.

1. Literature Review

1.1. *Candida* species – Candidiasis

Candida species are typically eukaryotic commensal yeasts that are members of the phylum Ascomycota and can be recovered from environmental, human, and other mammalian sources [1]. In humans, *Candida* species reside as part of the normal commensal microbial flora on mucosal surfaces of gastrointestinal and genitourinary tracts [1,2]. The genus *Candida* contains about 150 species, but only few of them, such as *Candida albicans*, *Candida tropicalis*, *Candida glabrata*, *Candida dubliniensis*, *Candida krusei*, *Candida parapsilosis* [3,4] and *Candida auris* [5] are implicated in human pathogenesis and have been associated with a wide range of human infections with significant mortality and morbidity [3,6,7]. The prevalence of *Candida* species is higher in pregnant, diabetic, elderly, or immunocompromised individuals, or in those who wear dentures or invasive catheters. They are also common in patients receiving antibiotic or corticosteroid treatment [6,8,9]. These microorganisms have a commensal relation with the host [8,10]. However, this relationship is characterized by a delicate balance and can thus become a parasitic relationship with the development of fungal infections designated by candidiasis [11,12]. The changes associated with this imbalance can result from alterations in the environment (disturbance in pH), use of antibiotics and/or changes in the immune system (caused by infection or immunosuppressive therapy) [12,13].

In general, human candidiasis manifests either as superficial, mucosal diseases, as systemic diseases or deep-organ infections [14–16]. Severe mucosal candidiasis, fall into two broad categories: chronic cutaneous mucosal candidiasis and chronic vaginal candidiasis [12,17]. The former is generally associated with weakening of the host's immune response, as seen in carriers of the human immunodeficiency virus and individuals such as hereditary immune deficiencies [18]. The second category is triggered by risk factors such as gestation, use of oral contraceptives, antibiotics, diabetes mellitus, among other. Severe systemic candidiasis is associated with neutropenia, leukemia, antineoplastic therapy or immunosuppression after transplantation [12,19].

The risk factors associated with candidiasis vary by species, being associated with several factors such as age, underlying disease, geographical differences, extensive use of traditional antifungals and failures in the control system [20].

In fact, the National Nosocomial Infections Surveillance System (NNISS) reports *Candida* species as the fourth most common nosocomial bloodstream pathogen. Mortality rates are estimated to be as high as 45 %, probably due to inefficient diagnostic methods and inappropriate initial antifungal therapies [2].

1.2. *Candida albicans*

Candida albicans is a diploid, polymorphic yeast existing in a unicellular yeast cell form, pseudohyphae and/or filamentous hyphae [21,22]. This microorganism can also switch between normal white yeast cell morphology and mating-competent opaque cell growth [1,22]. Its genome consists of eight pairs of chromosomal homologs, ranging in size from 0.95 to 3.3 Mb in size and comprising 16 Mb in total [23]. Despite its diploidy and clonal reproduction *C. albicans* is able to achieve a high rate of a genetic diversity in several ways, including recombination, chromosomal polymorphisms, and gene replacement, reflecting the plasticity of the genome [17,24]. This microorganism also exhibits frequent losses of heterozygosity as well as gross chromosomal rearrangements that may result in aneuploidy [1]. Though reproduction is predominantly asexual, the species can also utilise a para-sexual cycle [25,26]. In terms of fermentative growth ability *C. albicans* can grow in the presence of different subtracts such as glucose, maltose, and galactose although in the latter substrate its growth is variable [22].

Candida albicans differs in relation to other species of *Candida* mainly due to its pathogenicity level, being characterized by being a polymorphic diploid fungus, capable of rapidly changing the type of cell growth between yeast, pseudohyphae and/or true hyphae [1,27,28]. *Candida albicans* is the pathogenic species most frequently isolated and continues to be the main cause of candidiasis contributing to 50 % - 60 % of yeast infections in humans [29,30].

1.3. *Candida albicans*: virulence factors

The ability of *C. albicans* to cause infections in diverse host niches is supported by a wide range of virulence factors [31,32]. Several characteristics, including the morphological transition between yeast and hyphal/pseudohyphal forms (filamentation); adhesion and biofilm formation on biotic and/or abiotic surfaces; and hydrolytic enzyme secretion (proteases, phospholipases and lipases) are considered the most important virulence factors [33–35]. Additionally, the adaptability to environmental pH change, metabolic flexibility and stress response also play an important role in the virulence of C. *albicans* [33,34].

1.3.1. Adhesion and biofilm formation

An important virulence factor of *C. albicans* is its capacity to adhere and form biofilms on abiotic or/and biotic surfaces such as catheters, dentures (abiotic) and mucosal cell surfaces (biotic) that are the most common substrates [13,34,36].

Biofilms are complex three-dimensional structures that are composed of a core microbial cell community (either a single species or a mixed species) attached to host tissue or abiotic surfaces surrounded by an extracellular matrix (ECM) of polysaccharides that provide a shield or scaffold for the microbes beneath [36,37]. In addition, a biofilm provides protection against antimicrobials for the microbes associated with it, and thus biofilm-associated infections are more difficult to treat [38].

The formation of biofilms is based in a sequential process including adherence of yeast cells to the substrate, proliferation of these yeast cells, formation of hyphal cells in the upper part of the biofilm, accumulation of ECM and, finally, dispersion of yeast cells from the biofilm complex (Figure 1) [8,13]. The biofilm formation of *C. albicans* begins with the adhesion of yeast cells to a continuous population (Figure 1A) when the cell proliferation phase ensues and is followed by filamentation whereby the yeast cells begin to elongate and develop into filamentous hyphae [37]. The stage is characterized by being the initial phase of colonization when the cells change their morphology and invade either the host mucosal site or colonize abiotic surfaces in inert medical devices [13]. During this stage several hydrolytic enzymes such as proteinases, haemolysins, and phospholipase, are secreted, enabling the fungus to invade host tissue or other solid substrates [37,39]. After initiation occurs the development of biofilm consists on the cell proliferation and early-stage filamentation of adhered cells (Figure 1B) [13].

In the maturation step, the production of hyphae is a key feature accompanied by the secretion of polysaccharides for the ECM (Figure 1C) [13], where the major polysaccharides include α-mannan, β-1,6 glucan and β-1,3 glucan, raising a thick and structured architecture [34,37]. Moreover this structure origins the expression of drug efflux pumps and plasticity and, resistance to antimicrobial agents [33]. Fully mature *C. albicans´* biofilms have a mixture of morphological forms and consist of a dense network of yeasts, hyphae, and pseudohyphae in an ECM of, carbohydrates, proteins, and unknown components [34,40].

Finally, in the dispersal stage, some yeast cells have the ability to disperse from the mature biofilm and are then able to disseminate to distant sites to initiate a new cycle of biofilm formation (Figure 1D) [13]. The dispersal stage of biofilm is of immense clinical relevance, as the newly released cells from the mature biofilm located in either indwelling catheter or an infectious nidus are able to not only initiate new rounds of biofilm formation but also enter into the bloodstream to establish a distant focus of infection [37].
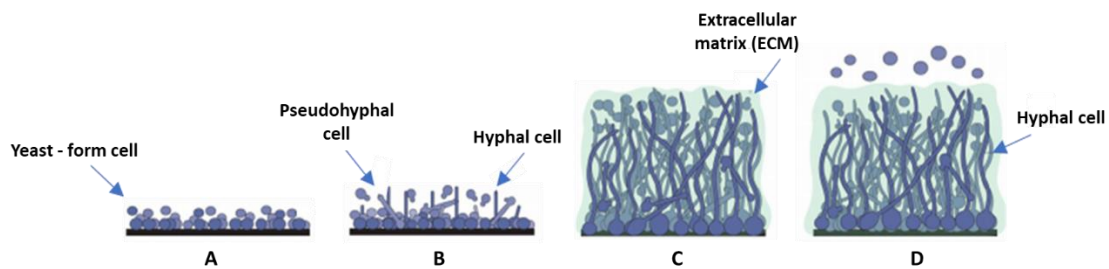
Figure 1. *Candida albicans* general stages of biofilm formation. **(A)** Adherence; **(B)** Initiation of biofilm formation; **(C)** Mature biofilm constituted by cells with diverse morphologies and extracellular matrix production; **(D)** Biofilm dispersion. Figure adapted from [8].

1.3.2. Secretion of hydrolytic enzymes

Candida albicans expresses three different classes of secreted hydrolases, namely, proteases, phospholipases, and lipases [34].

Among the hydrolytic enzymes that are secreted by *C. albicans* are the aspartic proteases, which represent one of the major virulence determinants as they have a potential role in pathogenicity through facilitating the invasion and counteracting the host defence system [41]. *Candida albicans* under and invasion process secretes aspartic proteases (Saps), encoded by a family of 10 *SAP* genes (sap1-10) which have a vital role in virulence of this pathogenic by degrading host proteins and invading tissues and organs as well as adhere to epithelial host tissue [34,41]. The effects of SAPs on *C. albicans* virulence can be supported by the activation of other genes such as *HWP1*. *HWP1* is a hyphal-specific adhesion gene that encodes the hyphal cell wall protein promoting *C. albicans* adhesion to different surfaces [42]. In addition, secreted hydrolases are thought to enhance the efficiency of extracellular nutrient acquisition [34,43].

The second group of secreted hydrolases, includes phospholipases (PL) that consist of a family of four different classes (A, B, C and D) [34,44]. The PL are enzymes that hydrolyse phospholipids to fatty acids, leading to host cell membrane damage [45]. In the fact the PL have been implicated

in host cell penetration, adhesion to epithelial cells invasion of reconstituted human oral epithelium and perhaps in the interaction with host signal transduction pathways [44].

Regarding lipases (Lip), they are involved on both the hydrolysis and the synthesis of triacylglycerols [46]. This third family of secreted hydrolases consists of 10 members (LIP1–10) [34,46], and a lip8Δ/Δ mutant had reduced virulence in a mouse model of systemic infection, supporting a role for these extracellular hydrolases in *C. albicans* pathogenicity [34].

1.3.3. Filamentation

Candida albicans is considered a polymorphic microorganism because it can grow either as ovoid-shaped budding yeast, as elongated ellipsoid cells with constrictions at the septa (pseudohyphae) or as true hyphae (Figure 2) [1,27,28,34].

A **B** **C**
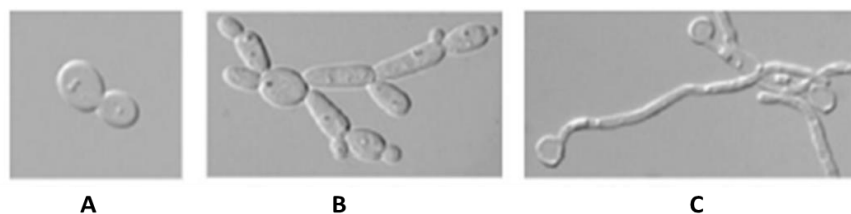
Figure 2. Different forms of morphological growth of *Candida albicans*. (A) Growth as yeast (blastoconidia); **(B)** Formation of pseudohyphae and **(C)** Formation of true hyphae. Figure adapted [28].

The transition from yeast to hyphae determines the change of *C. albicans* as commensal to pathogenic states and may lead to tissue infection, macrophage evasion, host-cell adhesion, and development of clinically relevant biofilm communities [32]. In the fact, this morphological transition which occur during growth is reversible and such physical plasticity is considered a key factor in virulence [14,35].

The polymorphism of *C. albicans* is a key factor in the virulence of this microorganism, and a range of environmental cues, for example pH, affect *C. albicans* ability to grow in all vegetative morphological forms: yeast (low pH <6), pseudohyphae and true hyphae (at high pH> 7) [22,28,33]. Indeed, several conditions, including starvation, the presence of serum or N-acetylglucosamine, physiological temperature and CO_2 promote the formation of hyphae [34,47]. In the fact the transitions between different morphological phenotypes represent a response of *C. albicans* to environmental changes and different cellular morphologies play different roles in the

processes of infection and adaptation to different host niches [48,49]. For example, the pH of the human blood and tissues is neutral or weakly alkaline, and the filamentation under these pH conditions would facilitate *C. albicans* cells to invade and colonize host tissues [50,51]. *Candida albicans* can also actively modify the environmental pH through the metabolism of available nutrients. For example, in the presence of glucose, the growth of *C. albicans* can acidify the medium by glycolysis. Alternatively, under the conditions of carbon deprivation, *C. albicans* uses amino acids as the carbon source and alkalinizes the extracellular environment by the production of ammonia [48,52]. This alteration of environmental pH affects yeast - filamentous growth transitions and may play a role in colonizing the host and causing infections [52–54].

1.3.4.   Filamentation: regulatory network of genes and genetic pathways

Great advances have been made in uncovering the underlying mechanisms of the morphologic regulation and the coordination and interplay between environmental factors and genes [15,51]. These advances in molecular studies of *C. albicans* are mainly due to genomic, transcriptomic, and proteomic techniques which provides the identification of different pathways and their key transcription characteristics [15,16,47].
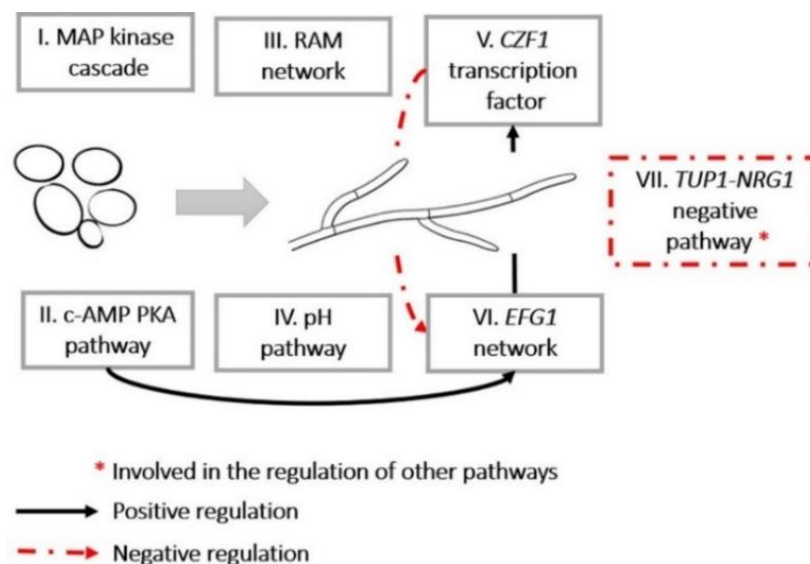
Figure 3. Illustrative representation of the pathways identified as involved in filamentation of *Candida albicans*.

Figure 3 shows the principal pathways of *C. albicans* morphogenesis, namely the mitogen-activated protein (MAP) kinase cascade (I), the cyclic adenosine monophosphate (cAMP)/protein kinase A (PKA) pathway (II), the polarized morphogenesis (RAM) network (III), the pH signalling (IV), the matrix embedding pathway through the *CZF1* transcription factor gene (V) and the genes associated with *EFG1* transcription factor (VI). *TUP1-NRG1*-mediated pathway (VII) was also identified as an important repressor of *C. albicans* filamentation.

Three differences pathways namely MAP kinase cascade, the cAMP/PKA and pH signalling will be described aiming to summarize the filamentation-associated genes and respective pathways.

1.3.4.1. MAP kinase cascade

MAPK pathway (Figure 4) is composed of conserved signalling cascades in eukaryotes that are important for dealing with a wide range of stimuli, including osmotic stress, oxidative stress, cell wall damage, and changes in glycosylation [34,55].
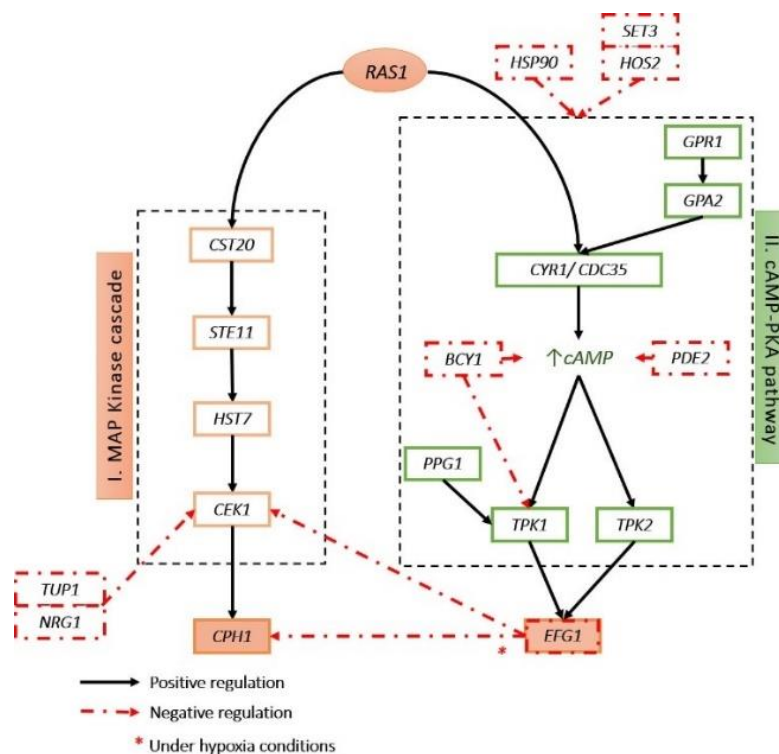
Figure 4. Illustrative representation of the MAP kinase cascade signal and cAMP/PKA pathway involved in filamentation of *Candida albicans*.

This signalling cascade is composed of a conserved module of three kinases: the MAP kinase kinase kinase (MAPKKK), the MAP kinase kinase (MAPKK) and the MAP kinase (MAPK) [51,55]. The signalling depends on three phosphotransfer steps, where the MAPKKK becomes phosphorylated and phosphorylates the MAPKK, which in turn phosphorylates the MAPK [55,56].

In *C. albicans*, three different MAPK pathways have been described: the Hog1-MAPK, the Mkc1-MAPK and Cek1/Cek2 [56,57]. All the MAPK signalling pathways serve as a pattern of cascades essential for *C. albicans* morphogenesis, but they are also required under different conditions and they are activated by different stimuli [55,56]. Among these MAPK pathways, *STE11-HST7-CEK1* composes the *CEK1* MAPK cascade (Figure 4) [55,58] and several studies have highlighted the involvement this pathway in morphogenesis and filamentation [56,58,59]. The activation of this signalling pathway begins with the interaction of *CDC42* with *RAS1* to activate MAPKKKK (*CST20*), which then triggers a subsequent phosphorylation of the MAPKKK (*STE11*) - MAPKK (*HST7*) -MAPK (*CEK1*/*CEK2*) cascade [51,56,57]. The cascade finally activates the downstream transcription factor *CPH1* which plays a major role in promoting filamentous growth and regulate the expression of several genes with a crucial function in the invasion of host cells or in biofilm formation [51,56].

1.3.4.2.   cAMP/PKA signalling

The cAMP/PKA pathway is highly conserved in eukaryotes (Figure 4) [51,60]. The cAMP/PKA signalling pathway regulates many features of *C. albicans* including virulence, morphological transitions, stress responses and metabolism [61–63], but it is one of the major pathways that positively regulate filamentation, involving the *EFG1* [64,65]. This signalling pathway is composed of a set of main components, include two Ras GTPases (Ras1 and Ras2) an adenylyl cyclase (Cyr1, also named as Cdc35) a low (Pde1) and a high (Pde2) affinity cyclic nucleotide phosphodiesterase and the PKA comprised of regulatory and catalytic subunits [61,62,64]. PKA consists of two catalytic and two regulatory subunits and is activated when cAMP binds to regulatory subunits to release the catalytic subunits [57,64]. In *C. albicans*, the PKA catalytic subunits have two isoforms encoded by *TPK1* and *TPK2* while the regulatory subunit is encoded by a single *BCY1* gene [62].

Ras1 cycles between an inactive GDP-bound and an active GTP-bound state and regulates filamentation in response to serum and other stimuli [64,66]. *RAS1* is activated by the guanine exchange factor Cdc25 and stimulates the adenylyl cyclase activity of Cdc35, which works with cyclase associated protein Cap1 to produce cAMP [62,64]. This results in an increase in the

intracellular concentration of cAMP which promotes its binding to the PKA regulatory subunits [66] (Bcy1) and induces a conformational change that leads to the dissociation and activation of PKA catalytic subunits [62,67]. These catalytic subunits then activate downstream targets, as the transcription factor *EFG1* [56,65,66].

1.3.4.3. pH signalling

The morphogenesis of *C. albicans* is mainly regulated by pH though a signalling pathway that converges upon the transcriptional regulator Rim101p (Figure 5), which is activated via C-terminal proteolytic processing in response to elevated pH [50,51,65]. The proteolytic processing of Rim101p is regulated by extracellular pH: acidic environments, rim101p is found in unprocessed full-length form, however environments with alkaline pH, is found predominantly in processed form that promotes changes in genetic expression [50,68,69].
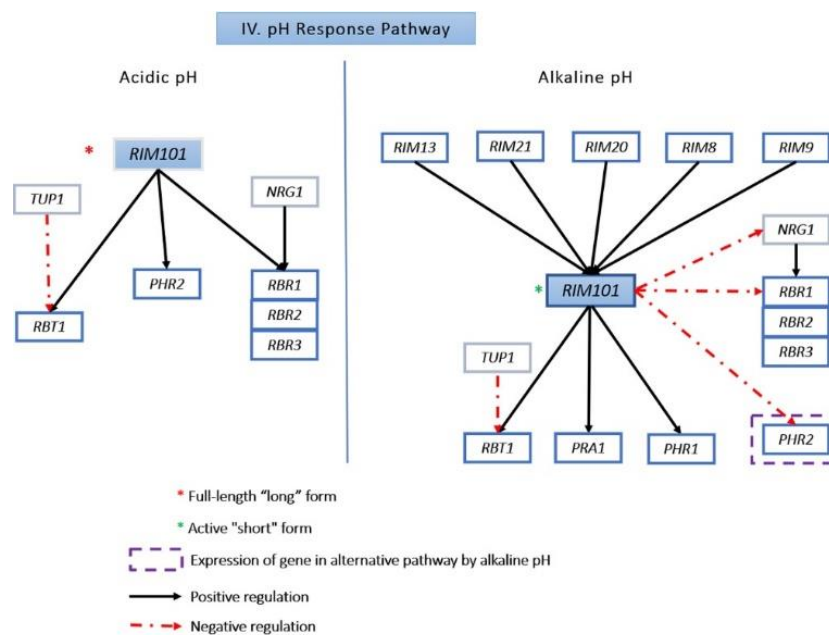
Figure 5. Illustrative representation of the pH response pathway in *Candida albicans*.

This proteolytic activation of Rim101p is controlled by a series of gene products, with *RIM101* itself being an alkaline-induced gene that depends on Rim8p, Rim13p and Rim20p for its induction [68,70]. In this signalling pathway, the external pH is detected by two transmembrane proteins, Dfg16p and Rim21p[51,70]. In neutral-alkaline conditions, Rim8 becomes hyperphosphorylated, leading to the endocytosis of this membrane complex and recruitment of the endosomal classification complexes necessary for transport (ESCRT) I, II and III [56,68]. Proteins Rim20 and

Rim13 are also recruited leading to the cleavage of the inhibitory C-terminal domain of Rim101, the final transcription factor of the Rim pathway [51,65,70]. Once activated, Rim101 migrates to the nucleus and regulates the expression of target genes involved in multiple cellular processes, including growth, iron metabolism, cell wall structure, transition from yeast to hypha, adhesion, and biofilm formation[34,70].

Thus, the *RIM101* signalling pathway directly regulates the repression of acid-induced genes and the activation of alkaline-induced genes (*PHR1/PHR2*), being the activation of filamentation dependent on the *EFG1* gene [56,65]. The activation of *EFG1* via Rim101p also leads to the activation of *TEC1*, which subsequently activates the expression of filament genes [65]. Studies have shown that *RIM101* does not play a significant role in the growth of *C. albicans* cells in acidic and alkaline environments, but mutants without *RIM101* have hyphae defects [48,50,69]. The pH response represents another example of the dynamic interaction and adaptation of *C. albicans* to its host environment [34,56] and all these features contribute to its remarkable capacity to co-exist as a commensal, or to prevail as a fungal pathogen in humans [34,48].

Candida albicans is thus a pathogen that exhibits a series of virulence factors that result in a drastic increase of human infections and associated to this increase infections arises the resistance of this microorganism to traditional treatments with antifungal [27,33,71]. Thus, it is urgent and imperative to unravel new alternative treatments, with new mechanisms of action and low toxicity to be applied on the control of *C. albicans* infections and antisense therapy can be a very promising alternative to deal with this global problem.

1.4.   Antisense Therapy

Antisense therapy (AST) represents a conceptually straightforward approach for disease's treatment [72]. With the mapping of the human genome, it is now possible to specifically target proteins independently, an approach that is potentially safer and more predictable for treating complex metabolic diseases than conventional, less-specific pharmacologic approaches [73,74]. This approach may be more specific than chemical inhibition and thus a potentially safer and predictable method for the treatment of complex diseases [75,76]. In fact, this technology represents a more specific treatment than chemical inhibition and is potentially a safer and more predictable method [75,77,78].

1.4.1. Antisense Oligomers: Mechanisms of Action

An antisense oligomer (ASO) is a single chain deoxyribonucleotide (usually 18-21 deoxynucleotides in length) that is complementary to target messenger RNA (mRNA) [74,79,80]. ASOs are chemically modified sequences, designed to specifically block the transfer of the genetic information for the protein synthesis by binding to a target RNA through Watson–Crick base pairing and thus selectively inhibit the expression of a single protein (Figure 6) [81–83].
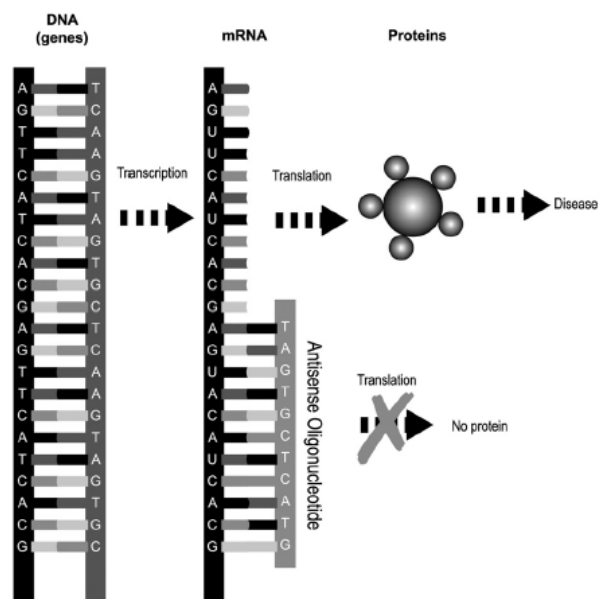
Figure 6. Antisense technology activity for inhibition gene expression. Representative scheme of the molecular basis involved in the principle of antisense technology. Figure adapted from [73].

For an ASO to recognize a specific target it must have a minimum length of 12 to 15 base pairs for an stable hybridization under physiological conditions [73,83,84]. After binding to their complimentary RNA sequence, ASOs inhibit the expression of specific target genes, by either splicing modifications or by recruiting RNase H leading to RNA degradation of RNA–DNA hetero-duplex, thus blocking the expression of the target gene [75,81].

In absence of ASO, the normal gene expression leads to a protein expression (Figure 7(1)). ASOs work through a variety of different mechanisms to achieve target manipulation (Figure 7), though these can be divided into two broad categories: the ASO that recruit RNase H for degradation (Figure 7(2)) and those that do not (Figure 7(3)) [83,85,86].
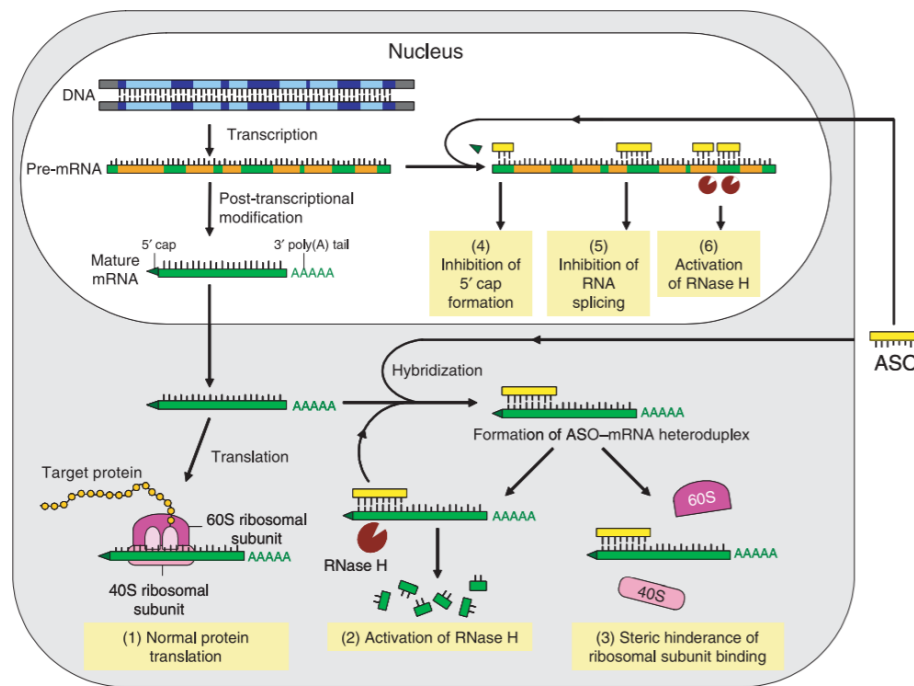
Figure 7. Antisense oligomers mechanisms of action. **(1)** Normal gene and protein expression in absence of ASO; **(2)** formation of an ASO-mRNA heteroduplex capable to induce RNase H activation, leading to selective degradation of bound mRNA or **(3)** steric interference of ribosomal assembly into cell cytoplasm. Alternatively, the ASO can enter the nucleus and regulate mRNA maturation **(4)** inhibition of 5´cap formation, **(5)** inhibition of mRNA splicing and **(6)**. Figure adapted from [86].

ASOs can activate an RNase H, which recognize RNA-DNA heteroduplexes, and induce the degradation of mRNA, but leaving the ASO intact [72–74]. More specifically, RNaseH1 is responsible for mediating RNA cleavage and as this enzyme releases intact ASO after cleavage of bound RNA, it permeates as soon as a single ASO catalytically cleaves many RNA molecules, further increasing ASO potency [87]. Since specificity of sequence has a direct effect in activity of RNase, it is important design an ASO with perfect match to the target sequence with more than 3 base pair [87,88].

Other ASOs that do not activate RNase H have an effect by binding tightly to the target mRNA, making them extremely useful for inhibiting translation, modulating splicing, and inhibiting microRNAs (miRNAs) [74,86]. In the first case, translation can be inhibited by blocking the movement of ribosomes down the transcript and/or inhibit the physical assembly of the 40S and 60S ribosomal subunits [87]. On the other hand, several studies demonstrated that ASOs have the ability to bind to the pre-mRNA structure and directly modulate splicing, both *in vitro* and *in vivo*, leading to exons inclusion or exclusion [89,90]. Another strategy, developed more recently, is based

12

on the design of ASOs against miRNA sequences, in an attempt to block miRNAs from binding to their own target mRNA molecules [91,92]. It is described that miRNA ASO has shown to be a promising therapy for effectively blocking miR-122 in hepatitis C infection in monkeys as well as human patients in phase II human trial [93,94].

1.4.2. Antisense Oligomers: Chemical modifications evolution

One of the major challenges for antisense approaches is the stabilization of ASOs, as unmodified oligonucleotides are rapidly degraded in biological fluids by nucleases [72,86]. Modifications to the ASO backbone and its sugar components have been developed leading to improvements in nuclease stability, thermodynamic binding stability and binding specificity, increasing efficiency for therapeutic application [85,95,96]. At the moment there are three different generations of nucleic acid mimics (Table 1) [73,97].
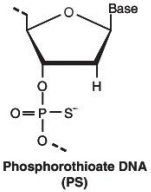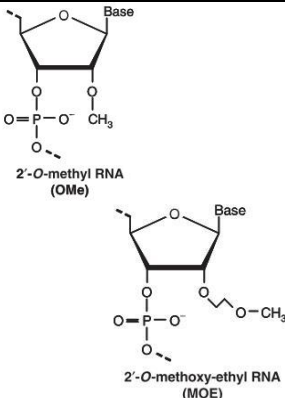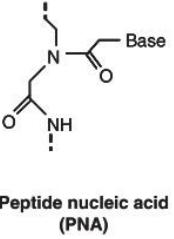
The first chemical modification applied to AST is still the most widely used: the phosphorothioate (PS) backbone [98] in which one of the non-bridging oxygen atoms in the phosphodiester bond is replaced by a sulphur atom [85,98]. This modification endows the ASO with enhanced stability and protection against nuclease degradation, leading to higher bioavailability of the oligonucleotide, enhance the attachment of ASOs to plasma proteins facilitating binding to cells and uptake into specific tissues, and the ability to recruit RNase H enzyme for target degradation [87,97,99]. A major disadvantage to the PS backbone modification is the potential inflammatory response generated at high concentrations [73] which have also been reported to produce non-specific effects by interactions with cell surface and intracellular proteins [86,97].
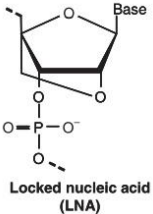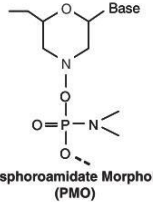
In order to eliminate nonspecific binding, enhance nuclease resistance, and increase binding affinity for target mRNA, second-generation ASOs with 2'-alkyl modifications of the ribose were developed [79,83]. 2'-*O*-Methyl (2'-OMe) and 2'-*O*-Methoxyethyl (2'-MOE) modifications of PS-modified ASOs are the two most widely studied second-generation ASOs [75,85,98]. This generation manifest less toxicity than PS-ASOs and a greater affinity and specificity for their complementary RNA sequence [73,85]. However, a limitation of ribose sugar modifications such as 2'-OMe is that they are unable to activate RNase H cleavage of the target mRNA [96,98] and the most used strategies to resolve this limitation has been to develop the 'gap' region, which consists in a longer central unmodified region (designated by 'wings') [97]. This chimeric 'gapmer'

ASO allows RNase H to sit in the central gap to execute target-specific mRNA degradation [74,96]; meanwhile 2' -modified "wings" further increase binding affinity and nuclease resistance while still allowing the center gap region to recruit RNaseH [87,96].

The third generation ASOs have emerged in recent years and displays improved target affinity, nuclease resistance, biostability and pharmacokinetics [73,85]. The development of this generation of ASO is based mainly on chemical modifications of the nucleotide furanose ring [86,96]. The three most studied ASOs third generation are peptide nucleic acid (PNA), locked nucleic acid (LNA) and phosphoroamidate morpholino oligomer (PMO) [72,74]. Peptide nucleic acid (PNA) is a synthetic DNA mimic in which the phosphodiester backbone is replaced with a flexible pseudopeptide polymer (N-(2-aminoethyl)glycine) and nucleobases are attached to the backbone via methylene carbonyl linkage [82,96]. Peptide nucleic acid is a non-charged nucleotide, which can hybridize complementary DNA or RNA with higher affinity and specificity than unmodified DNA-DNA and DNA-RNA duplexes [86,97]. In addition, PNA is not degraded by nucleases or peptidases, showing high biostability in biological fluids [86,99]. Locked nucleic acid (LNA) is a nucleotide conformationally as a restricted analogue of 2'-O-methyl-restricted RNA containing a 2'-O, 4'-C-methylene bridge in the β-D-ribofuranosyl configuration [82,100]. These compounds are nuclease resistant, non-toxic, and negatively charged [72]. In addition, this modification enhances its hybridization affinity towards target mRNA and DNA, with a substantial increase in the thermal stability of the duplexes and a much better potency [86,101]. These oligonucleotides as also show low toxicity in biological systems [102]. Phosphoroamidate morpholino oligomer (PMO) represents a non-charged ASO that were synthesized with a morpholino ring at the furanose ring site [82,96]. These molecules do not support RNase H activity, such that its ASO effect is primarily mediated by steric interference of ribosomal assembly resulting in translational arrest [82,86].

Table 1. Antisense oligomers chemical modifications and structures, their main features and disadvantages.

	Chemical Modification	Chemical structure	Description	Main features	Main disadvantages	Reference
First generation	Phosphorothioate (PS) backbone	Phosphorothioate DNA (PS)	The non-bridging oxygen atoms is replaced by a sulphur atom	-Improved nuclease resistance -Improved binding to plasma proteins -Ability to recruit RNase H	-Can cause immune response/cytotoxicity at high concentrations -Slightly reduced binding affinity with the mRNA target	[81,85,86,97]
Second generation	2'-*O*-methyl and 2'-*O*-methoxyethyl	2'-*O*-methyl RNA (OMe) 2'-*O*-methoxy-ethyl RNA (MOE)	PS-modified ASOs with 2'-alkyl modifications	-Improved binding affinity -Improved nuclease resistance - Less toxicity than PS-ASOs -2'OMe 'wings' allows the RNase H activation	-Does not support RNase H	[73,75,81,82,98]
Third Generation	Peptide nucleic acid	Peptide nucleic acid (PNA)	Synthetic DNA that phosphodiester backbone is replaced by *N*-(2-aminoethyl) glycine)	-Uncharged nucleotide -High binding affinity -Low toxicity -High nuclease resistance	-Low solubility -Poor uptake/pharmacokinetic properties.	[82,86,96,99]

	Name	Structure	Description	Advantages	Disadvantages	Ref
	Locked nucleic acid	Locked nucleic acid (LNA)	Sugar modification similar to 2'-*O*-methyl RNA.	-Increases thermal stability of the duplexes through hybridization affinity between DNA and mRNA target -Avoid nuclease degradation. -Better potency and low toxicity	-Higher toxicity than other modifications -Higher risk of a-specific binding -Higher propensity for self-annealing	[81,82,100–102]
	Phosphoroamidate morpholino oligomer	Phosphoroamidate Morpholino (PMO)	Non-charged ASO in which morpholino ring replaces the ribose sugar and Phosphoroamidate linkage replaces the phosphodiester bond	- Neutral charge -Improved binding affinity -Excellent nuclease resistance	-Poor uptake in cell nucleus -Poor pharmacokinetic properties	[82,85,86,96]

1.4.3. Antisense Oligomers: Applications

Over the last years, AST has emerged as a valid approach to selectively modulate gene expression [74,103]. This technology has been used to treat various neurodegenerative diseases, especially muscular atrophy where FDA approval has already been achieved. The application of ASOs has been shown to be a major challenge for the treatment of Alzheimer's disease and related dementias [97]. This molecular tool also excels in treating of oncological diseases [104]. In fact, several studies have been developed for the treatment of various types of cancer, such as cancer of the prostate [105,106], bladder [107,108], glioblastoma [109,110], among others [104].

The application of AST has also been recently applied to treat infections, as is the case with infections caused by gram-negative bacteria *Pseudomonas aeruginosa* in patients with cystic fibrosis [111]. Montagner [111] showed that antisense PNAs were able to inhibit bacteria-induced positive regulation of pro-inflammatory cytokines thereby protecting cells from a pro-inflammatory response induced by *Pseudomonas*. Previous studies [112] have also revealed that PNA antisense antibacterial oligomers targeting the translation initiation region of *ftsZ* mRNA (an essential bacterial gene involved in cell division) or *acpP* (an essential bacterial gene involved in the synthesis of fatty acids) of *P. aeruginosa* to reduce target mRNA levels, showing promising bactericidal activity.

However, the use of ASOs in the treatment of antifungal diseases, particularly in the control of infections caused by *C. albicans* still lacks information and the development of antisense molecules for clinical application. Nevertheless, a recent study [113] describes the development and application of the anti-*EFG1* 2'OMe oligomer to specifically control virulence factors of *C. albicans*. The anti-*EFG1* 2'OMe oligomer was able to significantly reduce the levels of expression of the *EFG1* gene and the translation of Efg1p protein, an important filamentation regulator gene in *C. albicans*.

Thus, although AST is a promising approach for the treatment of non-diseases in humans, the control of *C. albicans* infections is a problem that needs further investigation in order to be able to develop a credible and alternative methodology to control this pathogenic fungus.

2. *Candida albicans* growth and filamentation on simulated human body fluids under different pH*

2.1. Introduction

Candida albicans is one of the most important and common fungal opportunistic pathogens [2,46,114]. This microorganism is characterized as the major component of the human mycobiome of around 70 % of the healthy population, colonizing a variety of niches, such as gastrointestinal tract, mouth, and urinary and genital tract [8,31,32]. However, this species is capable of becoming pathogenic due to the changes in the composition of the microbiota [46,115], caused by alterations in pH, nutritional alterations, shifts in oxygen levels, antibiotic use, diseases, or immunosuppressant therapy [13].

The pathogenicity of *C. albicans* has been attributed to several virulence factors, such as the ability to switch from yeast to filamentous forms [33,34,46]. In fact, the cell responses to environmental changes, such as pH, allows *C. albicans* cells to take advantage of impaired immunity in debilitated patients and therefore facilitate the establishment of candidiasis [116,117]. Despite some controversy, there are scientific evidences that the environmental pH affects the ability of *C. albicans* to grow in all vegetative morphological forms, such as yeast (low pH <6), pseudohyphae and true hyphae (at high pH>7) [22,28,33]. The diverse niches that *C. albicans* inhabit vary prominently with respect to environmental pH [50]. For instance, the pH of the oral environment varies significantly between 6 to 7, meaning that it is slightly acidic, however the oral pH can reach a minimum of 5.3 and a maximum of 7.8 [118], resulting from changes in the diet, in the metabolism of other constituents of the microbiota and in the salivary flow [54]. In the urinary tract, changes in the amount or type of acid produced is patient dependent with a urine pH ranging from 4.5 to 8 [119].

Thus, the main goal this chapter was to deep our knowledge on *C. albicans*' behaviour on two simulated human body fluids (artificial saliva and urine) adjusted to different pH (pH 4, 5.8 and 7) in terms of growth and ability to develop filamentous forms.

2.2.   Material and Methods

2.2.1.   Simulated human body fluids

To mimic the human body fluids, artificial saliva (AS) and urine (AU) were used at different pH. AS (pH 4, 5.8 and 7) and AU (pH 4, 5.8 and 7) were prepared with slight modifications to that described by Silva et al (2010) and (2013) (Table 2). The pH of simulated body fluids was measured with a pH meter (C1010 Benchtop pH Meter, Cleaver Scientific) and adjusted using hydrochloric acid and/or sodium hydroxide. The Roswell Park Memorial Institute (RPMI; Sigma, St Louis, USA) buffered with 3-(N-Morpholino) propanesulfonic acid (MOPS; Sigma-Aldrich, St Louis, MO, USA) with 2 % of glucose, was also adjusted to pH 4, 5.8 and 7 and used as medium of control for all experiments. The pH of each fluid was also monitored at end of each experiment.

Table 2. Composition of saliva and artificial urine that mimic simulated human body fluids.

Simulated body fluid	Composition	Reference
Artificial saliva (AS)	2.0 g/L yeast extract	[120]
	5.0 g/L peptone	
	2.0 g/L glucose	
	0.35 g/L NaCl	
	0.2 g/L $CaCl_2$	
	0.2 g/L KCl	
	1.0 g/L mucin	
Artificial urine (AU)	0.65 g/L $CaCl_2$	[121]
	0.65 g/L $MgCl_2$	
	4.6 g/L NaCl	
	2.3 g/L Na_2SO_4	
	0.65 g/L $Na_3C_3H_5(CO_2)_3$	
	0.02 g/L $Na_2C_2O_4$	
	2.8 g/L KH_2PO_4	
	1.0 g/L NH_4Cl	
	1.6 g/L KCl	
	25.0 g/L urea	
	1.1 g/L creatinine	
	3.0 g/L glucose	

2.2.1. Organism and growth conditions

Candida albicans SC5314, the reference strain, was the microorganism used. The yeast belongs to the Biofilm Group collection, located at the Centre of Biological Engineering, University of Minho (Braga, Portugal). The identity of *C. albicans* strain was confirmed using a selective medium specifically CHROMagarTM *Candida* and by PCR-based sequencing with specific primers (ITS1 and ITS4) [122]. For all experiments, *C. albicans* strain was subcultured on sabouraud dextrose agar (SDA; Merck, Germany) and incubated for 24 h at 37 °C. A colony was obtained from SDA plate, resuspended in sabouraud dextrose broth (SDB, pH 5.6; Merck, Germany) and incubated at 37 °C for 18 h at 120 rpm. After this time, the cells' suspension was centrifuged for 5 min at 6000 g and 4 °C and washed twice with phosphate-buffered saline (PBS; pH 7, 0.1 M). Pellets were suspended in 5 mL of PBS and the cellular density adjusted for each experiment using a Neubauer chamber (Marienfild, Land-Konicshofem, Germany) to 1×10^6 cells ml^{-1}.

2.2.2. *Candida albicans* growth analysis

To evaluate *C. albicans* growth pattern, 10 mL of cells' suspensions (1×10^6 cells ml^{-1}) were prepared on AS (pH 4, 5.8 and 7) and AU (pH 4, 5.8 and 7) and incubated at 37 °C, over 30 h at 120 rpm. Cells' suspensions were simultaneously incubated on RPMI adjusted to pH 4, 5.8 and 7. All experiments were performed in triplicate and in a minimum of three independent assays.

2.2.2.1. Growth curves determination

Candida albicans cells' optical density (OD) was measured at 690 nm over the time using a microtiter plate reader (Microplate Photometer, Thermo Scientific). The specific growth rate was determined for each condition through the linear regression determination.

2.2.2.2. CFUs quantification

The number of cultivable cells for each condition was quantified after 24 h of incubation by colony forming units (CFUs) enumeration [123]. Thus, from each condition 1 ml of suspension was recovered and the pellets were washed once with PBS. Pellets were resuspended on PBS and serial dilutions were performed, plated into SDA, and then incubated at 37 °C. The total CFUs per mL (log_{10} CFUs/mL) were enumerated after 24 h of incubation.

2.2.2.3. Metabolic activity determination

An XTT (2,3-(2-methoxy-4-nitro-5-sulphophenyl)-5-[(phenylamino) carbonyl]-2H-tetrazolium hydroxide) (Sigma-Aldrich, USA) reduction assay was used to determine *C. albicans* cells' metabolic activity [123]. For that, after 24 h of growth 1 mL of each cells' suspension was harvested by centrifugation at 6000 g and 4 °C and washed once with PBS. An aliquot of 200 μL of a mixture of 100 ug/mL XTT and 10 ug/mL of phenazine methosulphate (PMS) (Sigma-Aldrich, USA) was added to the pellet and incubated at 37 °C for 3 h at 120 rpm. Optical density was measured at 490 nm using a microtiter plate reader. The metabolic activity was compared for each fluid and the absorbance values were standardized per number of CFUs determined previously (section 2.2.2.2). The ratio between the metabolic activity and number of CFUs was determined (Abs 490 nm/$\log_{10}$ CFUs).

2.2.3. *Candida albicans* filamentation analysis

The ability of *C. albicans* to develop filamentous on the different human simulated body fluids was evaluated by optical microscopy observation. For that, 24 h grown cells, prepared as described in section 2.2.2, were recovered by centrifugation for 5 min at 6000 g at 4 °C and washed once with PBS. The pellets were resuspended in 1 mL of PBS and the suspensions sonicated for 10 s at 30 % (Ultrasonic Processor; Cole-Parmer) to disaggregate cellular aggregates. The number of filaments was quantified using a Neubauer chamber by optical microscopic observation. The results were presented as the percentage of number of filaments: % of filamentation = (Filamented cells/total cells) *100.

In parallel, the morphology of cells was confirmed through observation on fluorescence microscopy (Olympus BX51 coupled with a DP71 digital camera; Olympus, Tokyo, Japan). For that, the cells were stained with 1 % (v/v) of calcofluor (Sigma-Aldrich, EUA) for 15 min in the dark. The laser DM 405/488/559/635 and the emission filters BA 430-470 (blue channel) were used, and the images were acquired with the program FluoView FV100 (Olympus). The filaments length' was also determined using the ImageJ Plug-in software.

2.2.4. Statistical analysis

Data were analyzed using analysis of variance (ANOVA) followed by the Turkey test to compare the mean values of different groups, using GraphPad Prism 6 software (GraphPad Software, San Diego, CA, USA). Data were expressed as the mean ± standard deviation (SD) of a least three independent experiments. All tests were performed with a confidence level of 95 %.

2.3. Results

2.3.1. *Candida albicans* growth on simulated human body fluids

The ability of *C. albicans* to grow as free cells on simulated human body fluids was analysed measuring optical density over 30 h on AS (pH 4, 5.8 and 7) and AU (pH 4, 5.8 and 7). *Candida albicans* cells were also grown on RPMI (pH 4, 5.8 and 7) as a control medium. Figure 8 shows that *C. albicans* is able to grow on both simulated human body fluids at all pH. Table 3 presents the specific growth rate of *C. albicans* under each condition, determined through linear regression (see figure AI.1 in annex I). The results revealed that *C. albicans* growth was slightly lower on AU than AS and RPMI. Analysing the behaviour of *C. albicans* on same simulated fluid, it was observed that growth pattern was slightly different depending on pH.
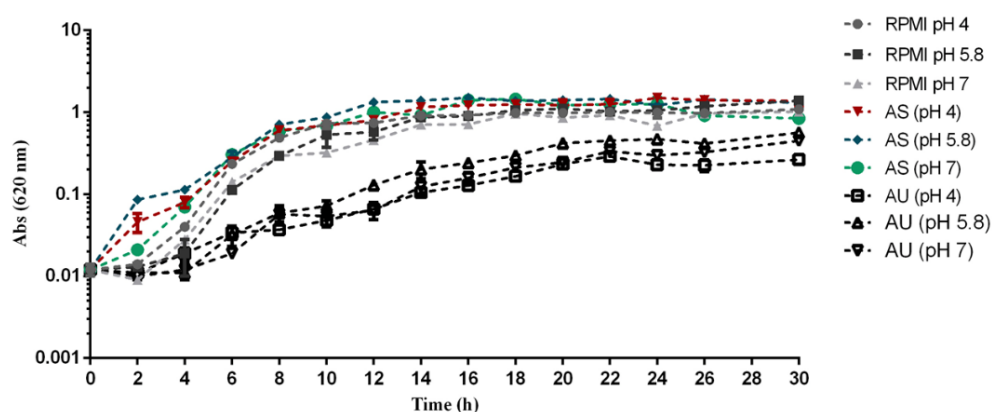
Figure 8. *Candida albicans* growth curves on simulated human body fluids. Growth curve of *C. albicans* SC5314 over 30 h on RPMI (pH 4, 5.8 and 7), AS (pH 4, 5.8 and 7) and AU (pH 4, 5.8 and 7). Error bars represent standard deviation.

In the case of AS, the profile of growth was similar for all pH tested, however the specific growth rate at pH 5.8 (0.158 h^{-1}) was slightly higher than pH 4 (0.094 h^{-1}) and pH 7 (0.101 h^{-1}). In case of AU, the specific growth rate was highest at pH 5.8 (0.014 h^{-1}), and it was similar at pH 4 and pH 7, with values of 0.005 h^{-1} and 0.007 h^{-1} (Table 3).

Table 3. *Candida albicans* specific growth rate on simulated human body fluids. Specific growth rate growth of C. albicans on RPMI (pH 4, 5.8 and 7), AS (pH 4, 5.8 and 7) and AU (pH 4, 5.8 and 7).

Fluid	Specific growth rate (h^{-1})
RPMI (pH 4)	0.095
RPMI (pH 5.8)	0.077
RPMI (pH 7)	0.052
AS (pH 4)	0.094
AS (pH 5.8)	0.158
AS (pH 7)	0.101
AU (pH 4)	0.005
AU (pH 5.8)	0.014
AU (pH 7)	0.007

It is important to address that the pH of each fluid was measured also after 24 h of incubation (see figure AI.2 in annex I) and were observed some variations in the pH values. On AS at pH 4, an increase of 2 OD values were observed, and at pH 5.8 an increase of 1.5 OD values. In the case of RPMI and AU at pH 4 a slight decrease on pH of 0.7 values was observed.

Figure 9 presents the number of cultivable cells on different simulated human body fluids after 24 h of *C. albicans* growth. The results revealed that *C. albicans* presented higher number of cultivable cells on AS than on AU and RPMI, however without statistical differences (P value >0.05). The condition where was observed the lower number of CFUs was AU pH 4 (P value <0.05). For the same body fluid, it was possible to infer that *C. albicans* presented slight differences in terms of CFUs at different pH, being slightly higher in AU at pH 5.8 and pH 7 compared to pH 4 (P value <0.05). In case of AS the number of CFUs was similar at all pH tested (pH 4, 5.8 and 7). In the case of RPMI studies, the number CFUs was lower at pH 7 compared to pH 4 and pH 5.8, however without statistical differences (P value >0.05).
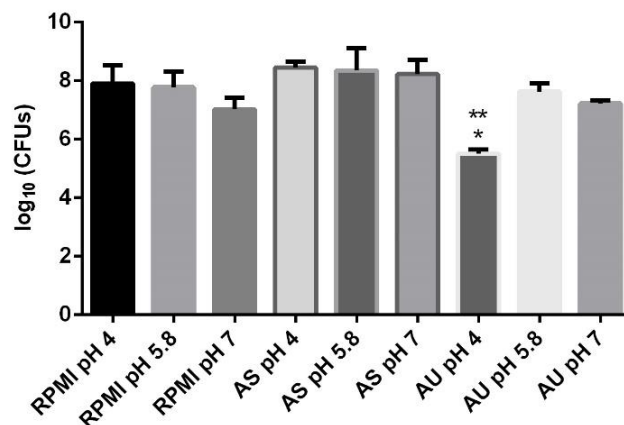
Figure 9. Number of *Candida albicans* cultivable cells on simulated human body fluids. Logarithm of CFUs obtained for planktonic growth of *C. albicans* SC5314 on RPMI (pH 4, 5.8 and 7), AS (pH 4, 5.8 and 7) and AU (pH 4, 5.8 and 7), at 24 h. Error bars represent standard deviation. *Significant differences between the same condition and different pH value; **Significant differences between RPMI and same fluid pH value (P value <0.05).

Candida albicans cells metabolic activity was determined through the XTT reduction assay and the values obtained (see figure AI.3 in annex I) were normalized by the respective number of CFUs (Figure 10). It was clear that *C. albicans* cells metabolic activity is fluid and pH dependent (Figure 10). *Candida albicans* showed slightly higher metabolic activity on AS than on AU despite with not statistically different, except in the case of pH 4 (P value <0.05). On AS and AU fluids, there are no significant differences in the values of metabolic activity for the different pH values, although on AU at pH 4 there is a slight decrease of metabolic cells activity. *Candida albicans* showed higher metabolic activity on RPMI at pH 4 and pH 5.8 when compared with the values on AS and AU at the same pH value (P value <0.05). Cells metabolic activity on RPMI decreases as the pH becomes more alkaline (P value <0.05).
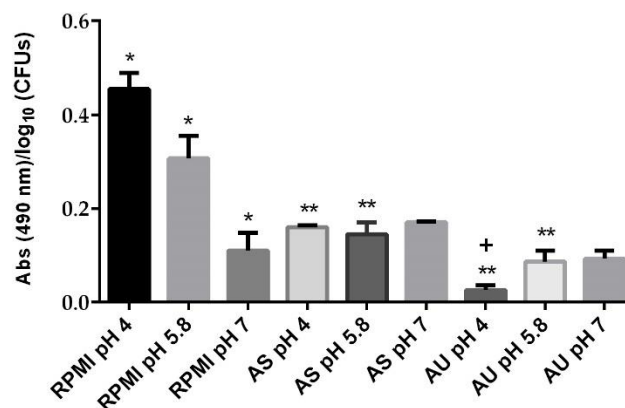
Figure 10. *Candida albicans* cells metabolic activity on simulated human body fluids. Metabolic activity determination by XTT reduction (Abs 490 nm/$\log_{10}$ CFUs) obtained for planktonic growth of *C. albicans* SC5314 on RPMI (pH 4, 5.8 and 7), AS (pH 4, 5.8 and 7) and AU (pH 4, 5.8 and 7), at 24 h. Error bars represent standard deviation. *Significant differences between the same condition and different pH value; **Significant differences between RPMI and same fluid pH value; ⁺Significant differences between different fluid and same pH value (P value <0.05).

2.3.2. *Candida albicans* filamentation on simulated body fluids

Candida albicans cells grown on different conditions were analysed by optical microscopy in order to evaluate their ability to grow as filamentous forms´ (Figure 11). The results revealed that *C. albicans* ability to form filaments is dependent on the fluid and also the pH. *Candida albicans* showed higher ability to form filaments on AU than AS at pH 5.8 (P value<0.05), however the percentage of filaments on AS at pH 7 was higher than AU at the same pH (P value <0.05). On AS at pH 4 and pH 5.8 the number of *C. albicans* cells grown as filaments was less than 1 % with significant increase at pH 7 for >25 % (P value <0.05). In contrast, *C. albicans* showed more ability to form filaments on AU at pH 5.8 (40 %) compared to pH 4 (9 %) and pH 7 (12 %) (P value <0.05). On RPMI at pH 7, *C. albicans* cells reached approximately 100 % of filaments, however as the pH value becomes more acidic, the percentage of filamentation decreases significantly (pH 5.8 - 70 % and pH 4 - 20 %) (P value <0.05).
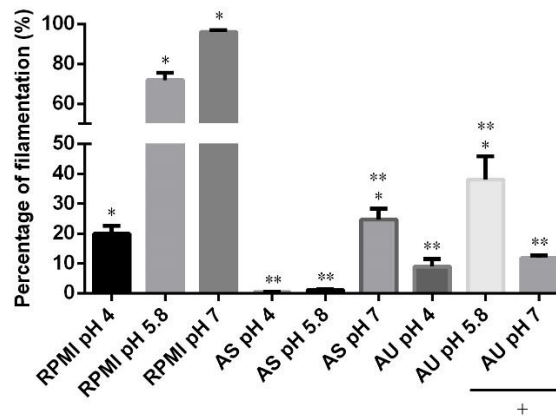
Figure 11. *Candida albicans* cells filamentation on simulated human body fluids. Filamentous forms percentage of *C. albicans* SC5314 on RPMI (pH 4, 5.8 and 7), AS (pH 4, 5.8 and 7) and AU (pH 4, 5.8 and 7), at 24 h. *Significant differences between the same fluid and different pH value; **Significant differences between RPMI and same fluid pH value; +Significant differences between different fluid and same pH value (P value <0.05).

The filamentous forms' length reached on the different simulated body fluids were quantified by fluorescence microscopy observation (Figure 12). The filamentous length was also fluid and pH dependent. It was clear, that the filaments length was higher on RPMI, than on AU and AS. On RPMI pH 7 (164 µm) and pH 5.8 (100 µm) the length was higher than on RPMI pH 4 (33 µm). In case of AS, the filaments were slightly higher at pH 5.8 (43 µm) compared to pH 4 (21 µm) and pH 7 (33 µm). On AU, the filaments length was also higher at pH 5.8 (52 µm) than at pH 7 (41 µm) and pH 4 (28 µm). On AS and AU at pH 4, the filaments length were the smallest comparing to all conditions.
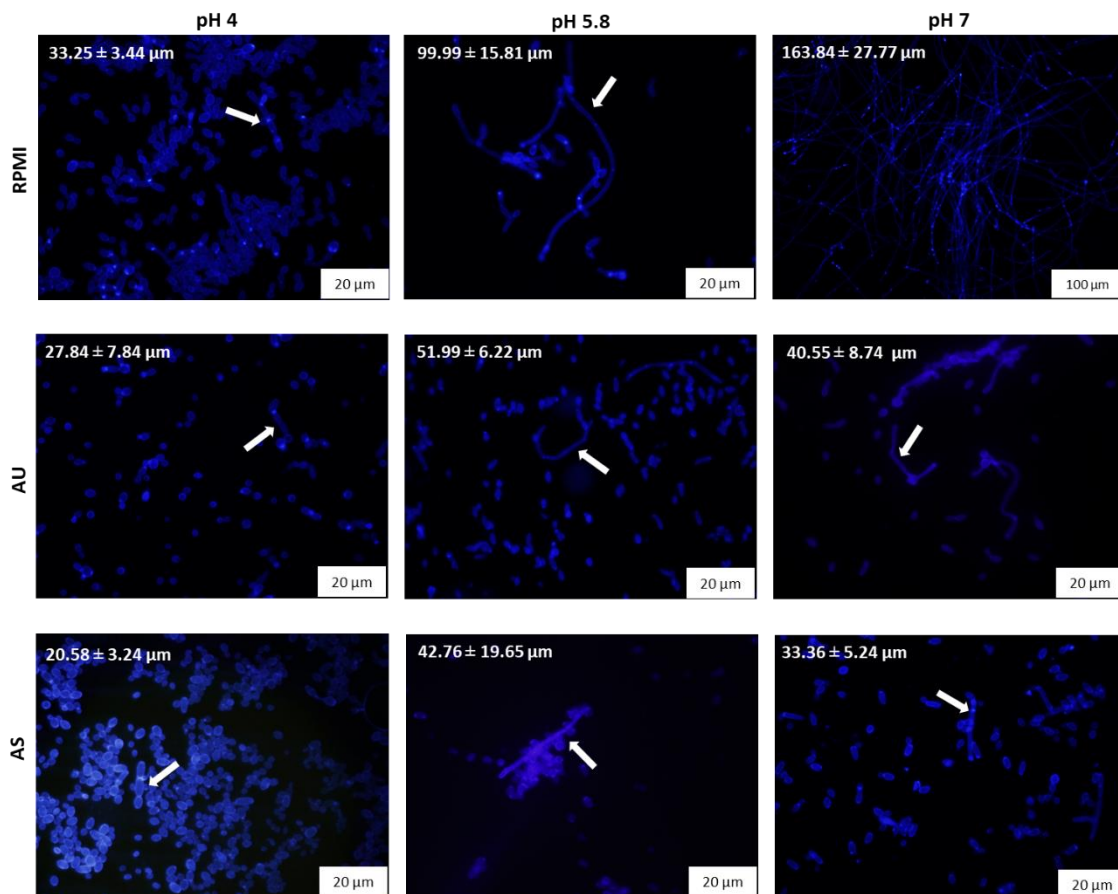
Figure 12. *Candida albicans* **cells morphology and filaments length on simulated human body fluids**. Fluorescence microscopy images of *C. albicans* SC5314 grown in RPMI (pH 4, 5.8 and 7), AS (pH 4, 5.8 and 7) and AU (pH 4, 5.8 and 7), at 24 h. Arrows highlight filamentous forms.

2.4.   Discussion

Candida species are the third most common microorganism responsible for health-care-related infections[114] causing hundreds of thousands of invasive infections with high mortality each year [29,30]. *Candida albicans* is still the most common of all *Candida* pathogens' species [31,46,114], colonizing different human niches including skin, oropharynx, lower respiratory tract, and gastrointestinal tract, and genitourinary system [8,31,32]. Its high success as a pathogen is related to their high capacity and plasticity to adapt to different fluids and environmental conditions of the human body [46,114]. The cellular response to external pH has also been described as advantage for colonization and invasion, affecting the ability of *C. albicans* to grow in all vegetative morphological forms, such as, yeast, pseudohyphae as well as true hyphae [22,28,33]. The switch

from a yeast to a filamentous form is a phenomenon that is directly related to the ability of transition from commensal fungus to a pathogenic state [28,31,124].

In order to deep the knowledge about the behaviour and adaptability of *C. albicans* on different human body niches, the present work aimed to study the ability of *C. albicans* to grown as free cells and to develop filamentous forms on two simulated human body fluids, namely saliva and urine at distinct pH.

The results revealed that *C. albicans* is able to grow on the human body fluids tested, however with different values of growth rates (Figures 8 and table 3). The growth of *C. albicans* was slightly higher in AS, compared with AU and with RPMI. In the case of AS the growth was very similar for all pH (4, 5.8 and 7), however with a slightly higher growth rate at pH 5.8 than pH 4 and 7 and even more than the observed in RPMI pH 7. Interestingly, it was observed that on AU, the behaviour of *C. albicans* was distinct, with a lower rate (for all pH tested) than on AS and even on RPMI. The pH of mimic fluids seems also to influence *C. albicans* growth, with the rate being slightly higher at pH 5.8 than pH 4 and 7 in the case of AU. Furthermore, the growth of *C. albicans* on RPMI was also dependent on pH, with a higher growth rate at pH 4 compared to pH 5.8 and 7. The number of cultivable cells (Figure 9) corroborate the results observed in terms of growth curves profile (Figure 8) with a slight increase in CFUs on AS at all pH compared with AU and RPMI at 24h of growth. On AU, the number of cultivable cells was slighter higher at pH 5.8 compared to other pH, specifically with statistical differences in case of pH 4 (P value <0.05). These results highlight the ability of *C. albicans* to adapt to diverse environments, which is fundamental to its pathogenesis [31,114]. It was clear that *C. albicans* cells are able to grow and survive on the two human body fluids, a fact that might explain the larger role of *C. albicans* colonization and disseminated infections [35,59].

To infer about the metabolic activity of *C. albicans* cells grown on human body fluids were used the XTT assay [123]. In this semiquantitative colorimetric method, XTT is reduced to an XTT formazan product by mitochondrial dehydrogenases of metabolically active cells [123,125]. The amount of the formazan product is measured using a spectrophotometer and is proportional to the number of metabolically active microbial cells [125]. XTT assays measure metabolic activity in a viable way, but not all cells are cultivable [126,127], so this semi-quantitative method may be related to other quantitative techniques, such as the CFUs assay [123,128]. Figure 10 represented the metabolic activity determined by the XTT test, which was normalized by the respective number of CFUs, once the metabolic activity values are cell dependent [123]. The results revealed that *C.*

albicans cells showed higher metabolic activity when incubated on RPMI pH 4 and pH 5.8 compared AS and AU for the same pH (P value <0.05). In case of AS, the metabolic activity was similar for both pH, as well as the CFUs number. For AU, the metabolic activity was also similar for both pH, although with a slight decrease in pH 4, however, the number of CFU decreases in pH 4 when compared to pH 5.8 and pH 7 with statistical differences (P value <0.05). It is interesting to highlight that the metabolic activity in RPMI decreases as the pH becomes more alkaline (P value <0.05).

The distinct behaviour of *C. albicans* observed on both simulated body fluids can be explained by the difference of components that constitute them. For instances, saliva consists of higher amount of proteins (peptone 5 g/L; mucin 1 g/L) that potentially serve as growth substrate for microorganisms under conditions of low external nutrient supply, promoting *C. albicans* proliferation [118,129,130]. In the composition of urine, there is also creatinine (1.1 g/L), a protein, despite its major constituent to be urea (25 g/L). Urea is considering the cause cell cycle delays and apoptosis in mammalian cells [131] perhaps it negatively affects the growth capacity of *C. albicans* in this medium. In this work it was verified that *C. albicans* showed more growth capacity and metabolic activity in AS compared to AU which may indicate that, when the environment is not favourable, *C. albicans* develop a stress response, resulting in less capacity growth and less metabolic activity.

The transition between yeast and hyphal growth forms is called dimorphism and it has been proposed that both growth forms are important for *C. albicans* pathogenicity [34,132]. It has been well investigated that pH have ability to control yeast to filamentous growth transition [50,51,59], where acidic pH represses the yeast to filamentous growth transition, and neutral and alkaline conditions promote the filaments growth [50,56,59]. In order to infer about the ability of *C. albicans* to filament on simulated body fluids, the number of filaments were enumerated, and the filaments analysed in terms of length. The results demonstrated that the ability of *C. albicans* to form filaments, is fluid and pH dependent (Figure 11). In case of AS, *C. albicans* presented a lower rate of filamentation when compared to AU and RPMI, at pH 4 and pH 5.8, however at pH 5.8 it presented higher length of filaments when compared with pH 7 in the same media (Fig. 12). The capacity to develop filaments in AU was higher at pH 5.8 than pH 4 and pH 7 and the length of the filaments was consistent with this filamentation rate. On RPMI it was evident that pH influences the ability of *C. albicans* to develop filamentous forms, since at pH 7, the rate of filamentation was almost 100 %, decreasing as the pH becomes less alkaline.

This study highlighted that the growth capacity of *C. albicans* on different simulated body fluids depends strongly on its composition, regardless of the pH condition but considering filamentation ability the behaviour of *C. albicans* was more complex. For example, when *C. albicans* grows on RPMI (control medium), the ability to form filaments is clearly dependent on pH, how has been described, alkaline conditions promoted filament shapes and acidic conditions repressed this morphology [50,59]. In fact, several studies have shown that a morphological transition of *C. albicans* is responsive to environmental pH, where pH ≥6.5 induce hyphae formation and pH <6 repress a yeast transition to hyphal morphologies [22,28,33]. The lower ability of *C. albicans* cells to filament on RPMI at pH 4 comparation to pH 5.8 and pH 7 corroborate this statement. However, in the case of simulated body fluids this ability is likely to be affected not only by the pH value but also by the compounds of the fluid. For instances, *C. albicans* showed higher ability to grow and revealed to have higher metabolic activity on AS however with lower ability to develop filaments. On AU, *C. albicans* showed less ability to grown and less metabolic activity in all conditions tested, although the ability to form filaments was higher at pH 5.8 compared to other values of pH.

From this study, it was possible to confirms that *C. albicans* cells have plasticity and adaptability to different human body fluids, which in part reflects the inherent physiological difference of *C. albicans* on the different human niches. This may be the justification for the high number of oral and urinary candidiasis.

3. Application of 2'-*O*MethylRNA antisense oligomers to control *RAS1* and *RIM101* virulence determinants and *Candida albicans* filamentation under different body fluids*

3.1. Introduction

As previously referred, antisense oligomers (ASOs) are simply short strands of nucleic acids that have a sequence that is complementary to the target mRNA and that bind to this target by means of standard Watson-Crick base pairing [81–83]. Up to now, there have been three generations of ASOs [86,133,134] with several chemical modifications in order to increase its nuclease resistance, reduce its toxicity, and enhance its affinity and half-life [135]. The 2'-*O*MethylRNA (2'OMe) sugar modification belongs to the second generation of acid mimics; however, these do not support RNase H activity (a specific degradation mechanism cleaving the target mRNA) [72,86]. An insertion of a longer central unmodified region, known as "gapmers", has been used as a popular strategy to allow that RNase to join and activate the degradation of the mRNA target [74,87]. Antisense therapy (AST) has emerged as a valid approach to selectively modulate gene expression [86,103] and has been used to treat various neurodegenerative diseases, [97], but poorly explored to treat infectious diseases, namely candidiasis [113].

The advances in the molecular studies of *C. albicans* have allowed the identification of a set of genes and cascades that are involved in the regulation of *C. albicans* transition from yeast to filament forms, one of the most problematic of virulent factors of *C. albicans*. Two of the most important cascades identified are the MAP kinase [51,55] and cAMP / PKA cascades [61–63], both regulated by the *RAS1* gene [56,62,64]. The pH signalling transcription factor *RIM101* gene, has been also associated with the ability of transition yeast-to-hyphae as response to different pH by *C. albicans* cells [56,68].

In this sense, this work is based on key hypothesis that if a pathogen´s genetic sequence of a specific gene is a determinant of virulence, as is the case of *RAS1* and *RIM101* genes, it will be possible to synthesize nucleic acid mimics that will be bind to

the correspondent mRNA produced and degraded it, and consequently, reducing its virulence phenotype (which, in this case, would be the filament development). Thus, the main goal of this work was to project and synthesis ASOs targeting the *RAS1* and *RIM101* mRNA and to validate, *in vitro*, its applicability.

3.2. Materials and methods

3.2.1. Gene's selection

The genes *RAS1* and *RIM101* were selected having in consideration the well-characterized regulatory network genes (Figure 4 and 5) involved in *C. albicans* filamentation. The sequences of *RAS1* (Orf19.1760; C2_10210C_A) and *RIM101* (Orf19.7247; C1_14340C_A) genes were obtained from *Candida* Genome Database (www.candidagenome.org).

3.2.2. Organism and growth conditions

For all experiments, the reference strain *Candida albicans* SC5314 was subcultured on sabouraud dextrose agar (SDA; Merck, Germany) and incubated in sabouraud dextrose broth (SDB; Merck, Germany) at 37 °C for 18 h at 120 rpm, as described in chapter 2. After incubation, the cells' suspension was centrifuged for 5 min at 6000 g and 4 °C and washed twice with phosphate-buffered saline (PBS; pH 7, 0.1 M). Pellets were suspended in 5 mL of PBS and the cellular density adjusted, for each experiment, using a Neubauer chamber (Marienfild, Land-Konicshofem, Germany), to $1x10^6$ cells ml^{-1}. Cellular suspensions were resuspended in 10 mL of RPMI adjusted to pH 4, 5.8 and 7 and incubated at 37 °C, over 30 h at 120 rpm. All experiments were performed in triplicate and in a minimum of three independent assays.

3.2.3. *RAS1* and *RIM101* expression analysis

3.2.3.1. Primer's design

The primers against the selected genes (*RAS1* and *RIM101*) were designed using the software Primer 3 web-based (http://www.bioinformatics.nl/cgi-bin/primer3plus/primer3plus.cgi). *PMA1* was used as *Candida* housekeeping gene (with a cycle threshold value media of 25±1). Table 4 describes the characteristics associated with each primer used in this work.

Table 4. Genes studied and respectively primer sequence, melting temperature (Tm) and amplification product.

Specie	Gene name	Systematic name	Sequence (5'-3')	Primer	Tm (°C)	Amplification (BP)
Candida albicans	RAS1	C2_10210C_A (orf19.1760)	5´-TGCAAATCAACAAGGTCAAG-3´	Foward	55	164
			5´-GACCAGAAGAAACACCTCCA-3´	Reverse		
	RIM101	C1_14340C_A (orf19.7247)	5´-TCCATGTCCCATTGAAGC-3´	Foward	57	169
			5´-TGTTGTTGCTTGGCCTCT-3´	Reverse		
	PMA1	C3_00720W_A (orf19.5383)	5´-TTGCTTATGATAATGCTCCATACGA-3´	Foward	57	66
			5´-TACCCCACAATCTTGGCAAGT -3´	Reverse		

3.2.3.2.   RNA extraction

To infer about how the pH can influence the expression of the *RAS1* and *RIM101*, the levels gene's expression was analysed by RT-PCR. For this, cells grown as described in section 3.2.2 were recovered at 12 h and 24 h. The cell suspensions were centrifuged during 5 min, at 6000 g and 4 °C, and washed once with PBS. After that, the cells were transferred for an RNase free collection tube and centrifuged at 8000 g and 4 °C for 5 min. The cells were ressuspended in lysis buffer (2-mercaptoethanol) and were disrupted with glass beads by sonication (6.5 V of velocity during 35 sec, twice, with intervals of 1 min on ice). After that, the supernatant was collected and added to an equal volume of ethanol 70 % (v/v) RNase free. The E.Z.N.A® Total RNA kit I (Omega, Bio-TEK) kit was used to complete total RNA extraction. The mix was transferred for the "Spin Cartridge" column and centrifuged at 12 000 g for 15 s at room temperature. After that, the column was washed with wash buffer I (700 µL) and subsequently, with buffer II (500 µL, twice). In each wash, the column was centrifuged at 12 000 g for 15 s and the fluid was discarded. Then, the spin cartridge was centrifuged at 12 000 g for 1 min to dry the column and consequently, was transferred to a new recovery tube. To remove the total RNA from the column, 40 µL of RNase-free water was added to the centre of the column and then centrifuged at 12 000 g for 2 min.

Finally, the RNA concentration was determined by optical density measurement in a nanodrop (NanoDrop 1000 Spectrophotometer Thermo Scientific®).

To avoid potential DNA contamination, the samples were treated with DNase (DNase I, Amplification Grade, Invitrogen). Thus, 4 µL of Mix (2 µL of DNase and 2 µL of Buffer) were added to each 10 µL of RNA sample and the samples were incubated for 1 h at room temperature.

3.2.3.3.   Synthesis of cDNA

To converse RNA into complementary DNA (cDNA), the Xpert cDNA Synthesis kit (Grisp) was used according to the manufacturer's instructions. For each sample, 10 µL of extracted RNA of defined concentration (15 ng/ µL) was added to 1 µL of the respective RNA, 1 µL of dNTPs, 1 µL of each Random Primer and 6 µL of RNase-free. Subsequently, the first synthesis cycle was performed, according to the following protocol: 5 min at 65 °C and 2 min on ice. After this initial step, for each sample, 2 µL of buffer, 0.25 µL of inhibitor RNA and 0.5 µL of reverse transcriptase were placed. The protocol used for the synthesis of cDNA was: 50 °C: 15 min; 85 °C: 5 min. After synthesizing the cDNA, it was quantified in the nanodrop (NanoDrop 1000 Spectrophotometer Thermo Scientific®).

3.2.3.4.   Quantitative Real-time PCR

The qRT-PCR (CFX96, Biorad) was used to determine the relative levels of messenger expression (mRNA) transcripts in RNA samples, using *PMA1* as *Candida* housekeeping gene. For that, 96-well microtiter plate was used to realize the quantitative PCR and in each well was added 2 µL of each sample of diluted cDNA (30 ng/µL), 5 µL of EvaGreen Supermix (Bio-Rad, Berkeley, CA, USA), 2.8 µL H$_2$O RNase free, 0.1 µL primer forward and 0.1 µL primer reverse. The negative control (NRT) was made for each cDNA sample in order to determine if there are DNA contamination.

The expression quantification of genes was performed by ΔCt [136] which was normalized to the housekeeping gene $\left(\triangle Ct = Ct \ (housekeeping \ gene) - Ct \ (target \ gene) \right)$ and also by *Pfaffl* [137] method $\left(ratio = \frac{(E*target)^{\Delta Ct_{target}(control-sample)}}{(E*ref)^{\Delta Ct_{ref}(control-sample)}} \right.$.

3.2.4.   AOS's design and synthesis

The sequence of *RAS1* and *RIM101* genes to design the respective ASOs were selected trough bioinformatics tools based on a search conducted at the *Candida* Genome Database (http://www.candidagenome.org/cgibin/compute/blast_clade.p. Several *RAS1* and *RIMI101*

sequences were aligned to ensure that will be selected a conserved region of each gene. A BLAST search was conducted to avoid similarity with any sequence of the *Homo sapiens* and other fungus species (http://blast.ncbi.nlm.nih.gov/Blast.cgi).

ASOs sequence was projected having in consideration some important characteristics, such as the gene region (the first 200 nucleotides), the size of ASO (between 12 and 20) [138], the melting temperature (Tm) (between 39 °C-42 °C), and the content of guanine-cytosine (GC) (around 50-60 %) [86,87]. The ASOs were designed based on second generation of nuclei acid mimics [85,86], using the 2'-*O*-Methyl (2'OMe) chemical modification [82,85]. The determination of melting temperature and GC content was determined by the online calculator (http://eu.idtdna.com/calc/analyzer) predicting also the ASO sequence with 2'OMe chemical modification (see table 3).

The anti-*RAS1* 2'OMe and anti-*RIM101* 2'OMe designed was purchased from Exiqon (Copenhagen, Denmark) according to the user own specifications, with custom added 5'- and 3'-modifications and then purified by HPLC. The original aliquots of ASOs were prepared to 100 μM and stored at -20 °C. The stock was prepared as an aliquot of 4 μM and stored a -20 °C in sterile ultrapure water.

3.2.5. Cytotoxicity assays

3.2.5.1. Cell culture

The 3T3 cell line (Fibroblast cells, Embryonic tissue, Mouse from CCL3, American Type Culture Collection) were cultured in Dulbecco's Modified Eagle's Medium (D-MEM, Biochrom, Germain) supplied by 10 % of fetal bovine serum (FBS, Sigma Aldrich) and 1 % of antibiotic containing P/S (penicillin and streptomycin) (Biochrom, Germain). Cells were stored at 37 °C with 5 % CO_2 and medium changed every two days in order to obtain a confluence approximately 80 %.

3.2.5.2. MTS assay

The cytotoxicity used assessed using the MTS (3-(4,5-dimethylthiazol-2-yl)-5-(3-carboxymethoxyphenyl)-2-(4-sulfophenyl)-2H-tetrazolium) method, which is based on the reduction of MTS tetrazolium compound by viable cells to generate a coloured formazan product that is soluble in cell culture media [139,140]. For that, 50 μL of 1×10^5 cells mL^{-1} of cells were placed in 96-wells plate and incubated for 24 h at 37 °C and 5 % CO_2. Different concentrations of ASO (10, 40, 100 nM) were prepared in D-MEM medium and 50 μL of each concentration was added to each well. In the case of negative control 50 μL of DMSO was added and in positive control 50 μL

of D-MEM medium was used. The plate was incubated for a further 24 h. After incubation, 10 μL of MTS solution (MTS (CellTiter 96® Aqueous One Solution Cell Proliferation Assay, Promega); 1 % of D-MEM without phenol) was added to each well and incubated during 1 h in the dark. Lastly, the absorbance was recorded at 490 nm with a microplate reader (Biochrom EZ Reader 800 Plus, Cambridge, England). All experiments were performed in triplicate and in a minimum of two independent assays.

3.2.6. AOS's effects on *Candida albicans*

3.2.6.1. Effect on filamentation

To evaluate the effect of ASOs (anti-*RAS1* 2'OMe and anti-*RIM101* 2'OMe) on *C. albicans* filamentation, cells suspensions were adjusted to 1×10^6 ml^{-1} cells and resuspended in 10 mL in RPMI (pH 4, 5.8 and 7) in the presence of 40 nM of each ASO. As a control *C. albicans* cells were grown under the same conditions but without ASOs. Each suspension was incubated at 37 °C for 24 h at 120 rpm. The ability of *C. albicans* to form filamentous forms were evaluated using the methodology described in section 2.2.3 (chapter 2) at 12 h and 24 h of incubation. The results were presented as the percentage of inhibition on the number of filaments: % of filamentation inhibition = [(% of cells in filamented on control) - (% of cells filamented in presence of ASO)] / [(% of cells in filamented on control) *100.

In parallel, the morphology of cells was confirmed through observation on fluorescence microscopy (Olympus BX51 coupled with a DP71 digital camera; Olympus, Tokyo, Japan) as described in section 2.2.3 of chapter 2 and the length of the filaments determined using the ImageJ Plug-in software.

3.2.6.2. Effect on gene expression

In order to infer about the direct effect of ASOs (anti-*RAS1* 2'OMe and anti-*RIM101* 2'OMe) in the levels of *RAS1* and *RIM101* genes expression, quantitative real time PCR studies were performed. For that, cells suspensions of *C. albicans* were prepared as described in section 3.2.5.1. After 12 h and 24 h of incubation the RNA was extracted, cDNA synthetized, and qPCR performed as referred in section 3.2.2. All experiments were performed in triplicate and in a minimum of three independent assays.

3.2.7. Performance and stability of ASOs on simulated body fluids

3.2.7.1. ASOs individual performance

To study the stability and performance of the ASOs on simulated body fluids, *C. albicans* cells were incubated on saliva and artificial urine. For that, *C. albicans* cells were incubated in AU (pH 4 and 5.8) and AS (pH 7) (see composition on Table 2) in the presence of 40 nM individual doses of each ASOs, during 12 and 24 h as described in section 3.2.5.1. The results were presented as the percentage of reduction in the number of filamentous cells.

3.2.7.2. ASOs combined performance

In order to study the combined effect of the ASOs on *C. albicans* filamentation, the yeast cells were incubated simultaneously in the presence of 40 nM of anti-*RAS1* 2'OMe and anti-*RIM101* 2'OMe on AU pH 5.8 and AS pH 7. The assays were performed as described in section 3.2.5.1.

3.2.8. Statistical analysis

Data were analyzed using analysis of variance (ANOVA) followed by the Turkey test to compare the mean values of different groups, using GraphPad Prism 6 software (GraphPad Software, San Diego, CA, USA). Data were expressed as the mean ± standard deviation (SD) of a least three independent experiments. All tests were performed with a confidence level of 95 %.

3.3. Results

3.3.1. Influence of pH on *C. albicans RAS1* and *RIM101* genes expression

To understand how pH can influence the expression of *RAS1* and *RIM101*, the levels of gene expression were quantified by RT-PCR (Figures 13A and B, respectively) at 12 h and 24 h of growth on RPMI at pH 4, 5.8 and 7. Figure 13A and B presents the levels of *RAS1* and *RIM101* expression. The results showed that both genes were expressed under all conditions, however in a distinct level. No significant differences were observed for both genes at 12 h of incubation for all condition's assays (Figure 13 A and B). The level of expression of *RAS1* was superior at 24 h comparatively at 12 h on RPMI pH 5.8 and RPMI pH 7 (P value <0.05). The analysis showed that the highest level of expression (approximately 100 %) was achieved for alkaline condition (pH 7) (P value <0.05). Likely for *RIM101* at 24 h the levels of expression increased significantly, particularly at pH 7 where was observed the highest levels of expression (around 650 %; P value <0.05). It is important to address that both genes presented higher levels of expression at pH 7 (Figure 13 A

and B), condition where *C. albicans* reaches values near to 100 % of filamentation (Figure 11, chapter 2).
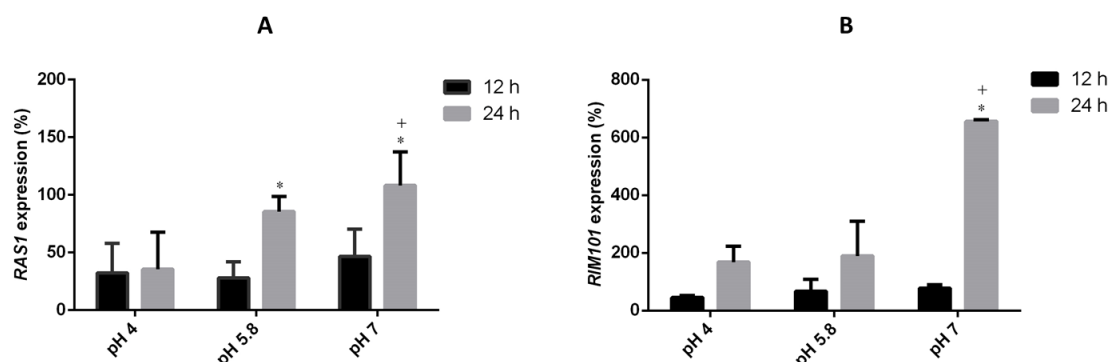
Figure 13. Influence of pH on *Candida albicans RAS1* and *RIM101* genes expression. (A) *RAS1* and **(B)** *RIM101* levels of gene expression of *C. albicans* SC5314 grown on RPMI (pH 4, 5.8 and 7), at 12 h and 24 h. *Significant differences between 12 h and 24 h for the same condition; +Significant differences between RPMI pH 4 and other pH values for the same time (P value <0.05).

3.3.2. Anti-*RAS1* 2'OMe and anti-*RIM101* 2'OMe characteristics

The second generation of nucleic acid mimics, the 2'OMe chemical modification, was the base for the design of anti-*RAS1* and anti-*RIM101* oligomers. A set of sequences for each gene, with low similarity with *Homo Sapiens* and high specificity for *C. albicans*, were previously selected (see table A.II.1 in annex II) using bio-informatic tools.

It is assumed [86,87] that for reaching an optimal performance of the ASOs, they must be projected with melting temperatures (Tms) around 39 °C-42 °C and with content of guanine-cytosine (GC) of approximately 50 % to 60 %, in order to increase the binding affinity for target mRNA and its stability in the human body. Furthermore, several studies have shown that ASOs with sizes between 12 and 20 nts (nucleotides) are normally the cause of an ideal hybridization performance [81,134].

Taking in to account these features, the ASOs synthesized were: **mUmGmG TTA AAC GGmG mAmU** (with 42.0 °C of Tm; 42.9 % of GC; 14 nts) against *RAS1* and **mGmGmU GAC GTA GmCmAmU** (with 44.9 °C of Tm; 53.8 % of GC; 13 nts) against *RIM101* (Table 5).

Table 5. Sequences of Anti-*RAS1* 2'OMe (m), and Anti-*RIM101* 2'OMe (m), with respective size, melting temperature (Tm) and GC content (% GC). The design has made by the OligoAnalyzer 3.1.

Gene	Sequences	Length	Tm (°C)	% GC
RAS1	mAmUmG GTT AAA GC GmGmAmU	15	42.6	40
	mUmGmG TTA AAC GGmG mAmU	**14**	**42.0**	**42.9**
	mUmCmA ATA GTT GGmG mUmC	14	42.5	42.9
	mGmCC AGA TAT TCT TmCmU	15	44.4	40
RIM101	mAmCmU TGC ACC GmGmUmA	13	48.6	55.8
	mGmAmG GAA TGG GGmA mCmU	14	48.2	57.1
	mGmGmU GAC GTA GmCmAmU	**13**	**44.9**	**53.8**

m - 2'*O*-Methyl RNA; **A -** Adenine; **T -** Thymine; **C** - cytosine; **G -** Guanine; **U -** Uracil.

3.3.3. Anti-*RAS1* 2'OMe and anti-*RIM101* 2'OMe cytotoxicity evaluation

In order to infer about the cytotoxicity of each ASO, the viability of fibroblast cells (3T3 cell line) in the presence of different concentrations of anti-*RAS1* 2'OMe and anti-*RIM101* 2'OMe was determined using the MTS assay (Figure 14A and B).

The results revealed that different concentrations of both ASOs are not cytotoxic. None of the concentrations tested led to a percentage of human cell viability below 70 % [Anti-*RAS1* (10 nM: 89 %; 40 nM: 84 %; 100 nM: 82 %); (Anti-*RIM101* (10 nM: 77 %; 40 nM: 80 %; 100 nM: 78 %)] [141]. Have in consideration these results, it was decided to use ASOs at 40 nM for the subsequent experiments, since was the intermediate concentration value without cytotoxicity.
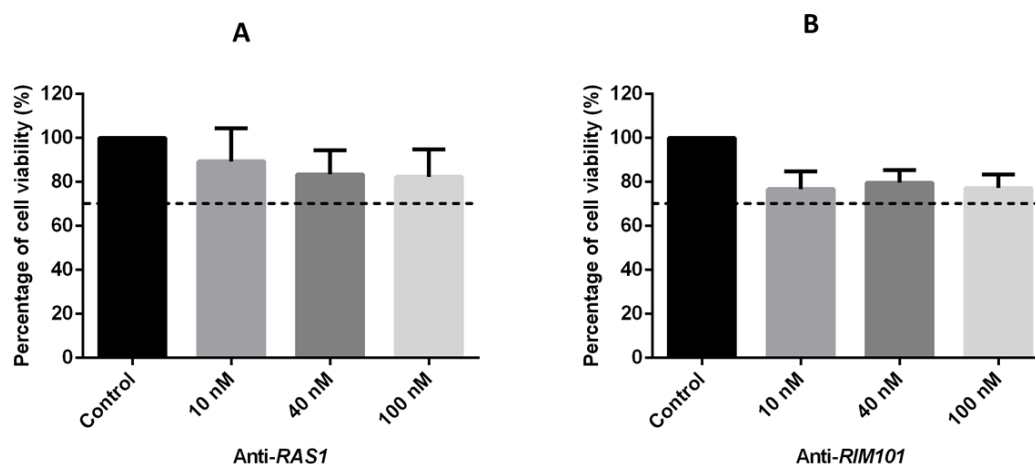
Figure 14. Cytotoxicity of antisense oligomers. (A) Anti-*RAS1* 2'OMe **(B)** Anti-*RIM101* 2'OMe. Percentage of 3T3 cell viability in the presence of different concentrations of antisense oligomers (10, 40, 100 nM). Error bars represented standard derivation.

3.3.4.   Effect of anti-*RAS1* 2'OMe and anti-*RIM101* 2'OMe on *C. albicans*

The effect of anti-*RAS1* 2'OMe and anti-*RIM101* 2'OMe on *C. albicans* cells was evaluated in terms of genotype (gene expression inhibition) and phenotype (reduction on number and length of filamentous).

3.3.4.1.   Anti-*RAS1* 2'OMe effects

Figure 15 showed that anti-*RAS1* 2'OMe was able to reduce the levels of gene expression in all conditions tested at 12 h (Figure 15A) and 24h (Figure 15B) (P value <0.05) of *C. albicans* grown. After 12 h and pH 7 it was observed the highest level of gene expression reduction (around 95 %), however, lower levels of reduction were obtained for the lower pH. After 24 h and at pH 7, the levels of gene reduction decrease to 24 %. Contrarily, it was observed an increase on anti-*RAS1* 2'OMe effect at pH 5.8 and 4, with values of reduction around 54 % and 42 %, respectively. It is important to address that in parallel with the reduction on levels of gene expression it was also verified a significant reduction on *C. albicans* filamentation (Figure 15C). The reduction on number of cells filamented increased from 12 to 24 h in RPMI pH 4 (6 % to 26 %) and pH 7 (17 % to 39 %) (P value <0.05). At pH 5.8 de levels of reduction remain at same values, around 38 %, for both periods of *C. albicans* cells growth.
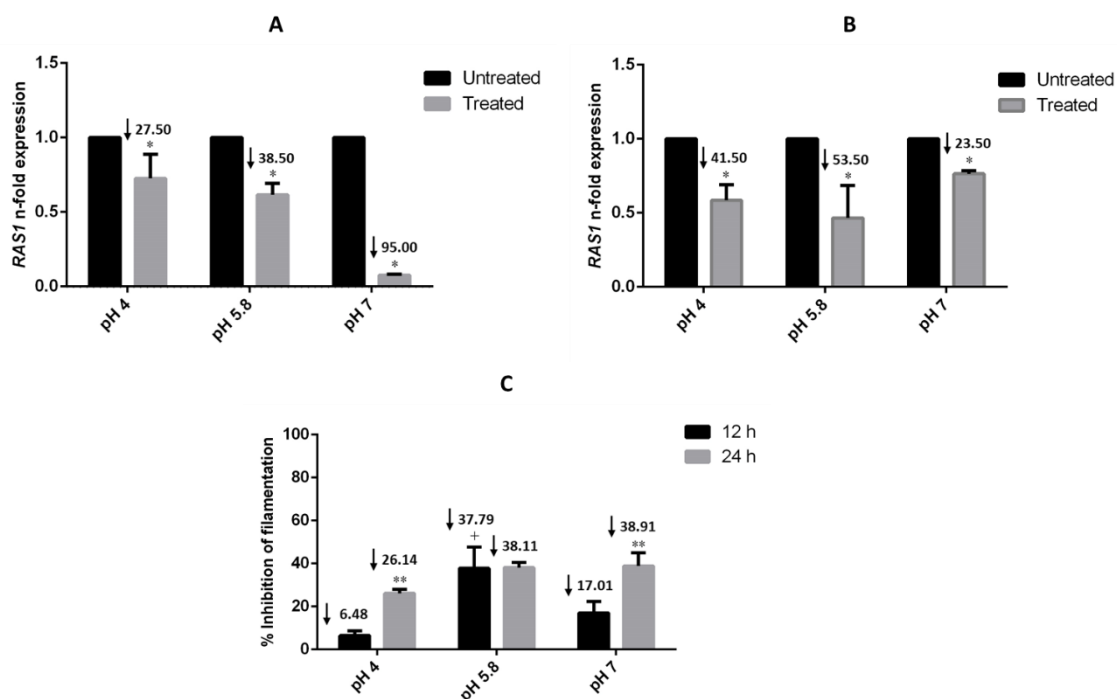
Figure 15. Anti-*RAS1* 2'OMe effects on *Candida albicans*. Levels of *RAS1* gene expression obtained by the *Pfaffl* method, at 12 h **(A)**; 24 h **(B)** and **(C)** percentage of inhibition of *C. albicans* cells filamented after treatment with 40 nM of anti-*RAS1* 2'OMe, in RPMI under different pH values (pH 4, 5.8 and 7). Controls (untreated) were prepared only with cells on RPMI (pH 4, 5.8 and 7) (without ASO). Error bars represent standard derivation. *Significantly differences between controls and cells treated with 40 nM of anti-*RAS1* 2'OMe; **Significant differences between 12 h and 24 h for the same condition; ·Significant differences between RPMI pH 4 and other pH values for the same time point (P value <0.05).

It is clear that the anti-*RAS1* 2'OMe is not only able to reduce the number of filamentous cells but is also able to reduce the filamentous forms' length (Figure 16), particularly for pH 7, where it was observed a reduction from 99 µm to 63 µm at 12 h and a reduction from 165 µm to 88 µm after 24 h of treatment.
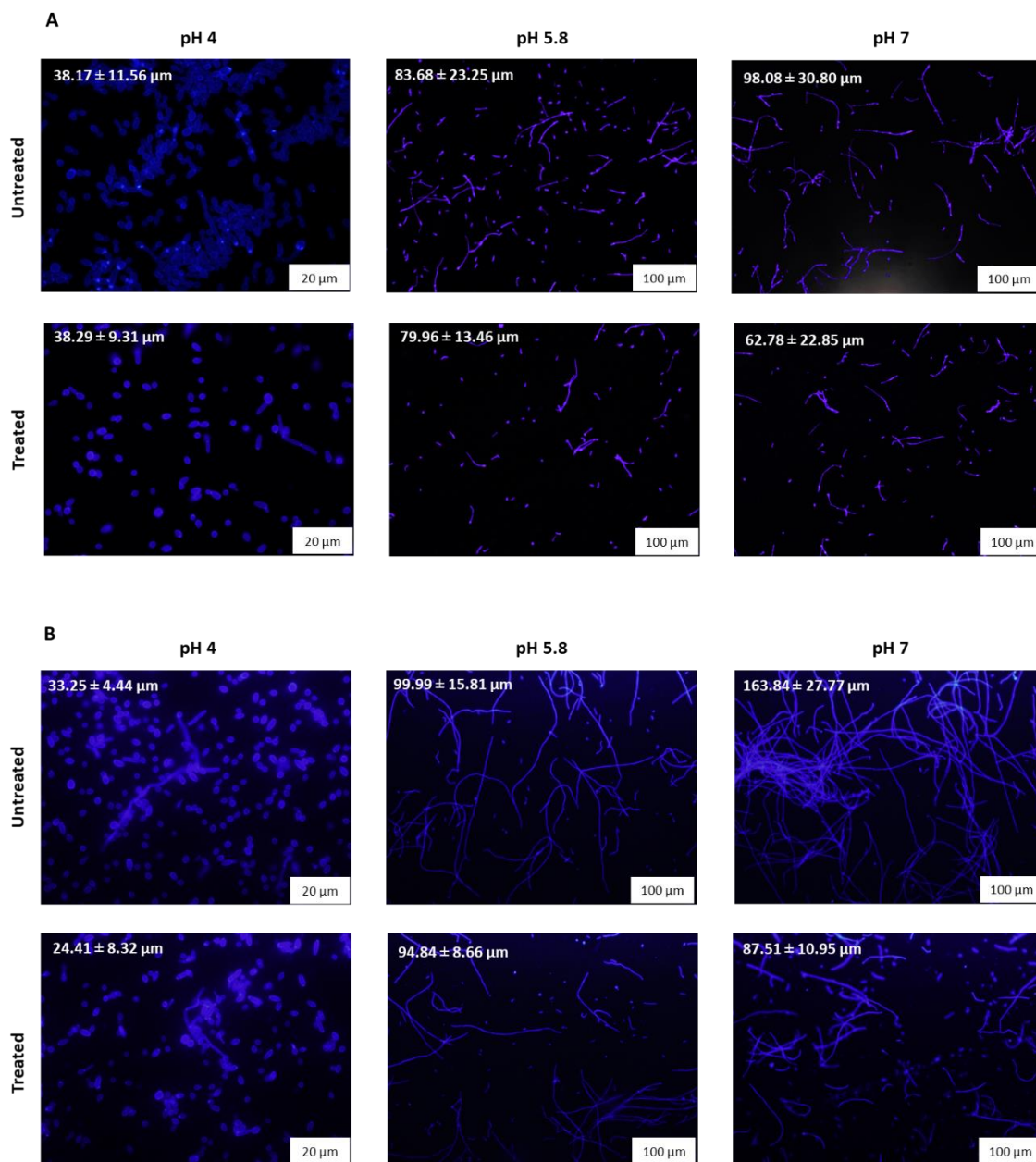
Figure 16. Anti-*RAS1* 2'OMe effect on *Candida albicans* cells length. Fluorescence microscopy images of *C. albicans* cells grown in RPMI (pH 4, 5.8 and 7) in the presence of 40 nM of anti-*RAS1* 2'OMe, at 12 h **(A)** and 24 h **(B)**. Controls were prepared only with cells grown in RPMI (pH 4, 5.8 and 7) (without ASO).

3.3.4.2.   Anti-*RIM101* 2'OMe effect

Figure 17 shows that anti-*RIM101* 2'OMe was also able to reduce the levels of gene expression in all conditions tested at 12 h (Figure 17A) and 24 h (Figure 17B) (P value ≤0.05) of *C. albicans* growth.
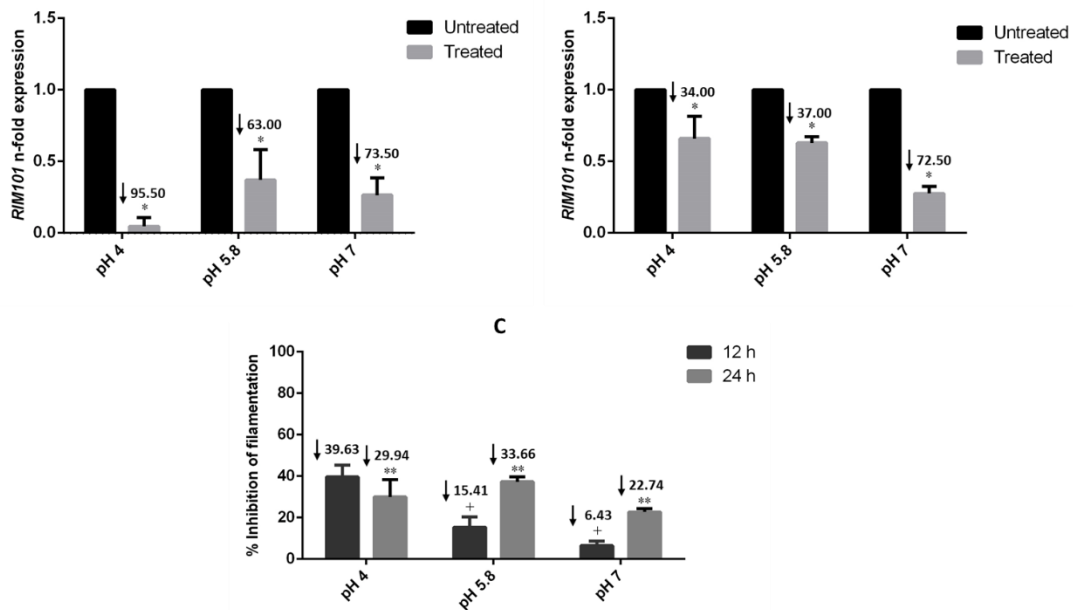
Figure 17. Anti-*RIM101* 2'OMe effects on *Candida albicans*. Levels of *RIM101* expression obtained by the *Pfaffl* method, at 12 h **(A)**; 24 h **(B)** and **(C)** percentage of inhibition of *C. albicans* cells filamented after treatment with 40 nM of anti-*RIMI101* 2'OMe, in RPMI under different pH values (pH 4, 5.8 and 7). Controls (untreated) were prepared only with cells in RPMI (pH 4, 5.8 and 7) (without ASO). Error bars represent standard derivation. *Significantly differences between controls and cells treated with 40 nM of anti-*RIMI101* 2'OMe; **Significant differences between 12 h and 24 h for the same condition; ⁺Significant differences between RPMI pH 4 and other pH values for the same time point (P value <0.05).

It is important to address that despite it was observed a reduction on levels *RIM101* of expression for all conditions, it was more pronounced 12 h (Figure 17A). The treatment of *C. albicans* cells with anti-*RIM101* 2'OMe led to reduction levels of gene expression of around 95 % at pH 4, 74 % at pH 7 and the approximately 63 % at pH 5.8. In general, the effect of anti-*RIM101* 2'OMe at 24 h were significantly lower, achieving levels of reduction of 34 % at pH 4 and 37 % at pH 5.8. Anti-*RIM101* 2'OMe maintains its performance with around 73 % of reduction at pH 7 in both time points analyzed. It is evident that anti-*RIM101* 2'OMe was not only able to control the levels of gene expression but it is also able to reduce the number of *C. albicans* filamented (Figure 17C). The levels of percentage reduction increased from 12 h for 24 h on RPMI pH 5.8 (15 % to 34 %) and pH 7 (6 % to 23 %) (P value <0.05). On the opposite, at pH 4 the levels of reduction decreased from 40 %, at 12 h, to 30 % at 24 h (P value <0.05).

It is evident that, like for anti-*RAS1* 2'OMe, the anti-*RIM101* 2'OMe was also able to reduce the number of cells filamented and the filaments' length (figure 18).
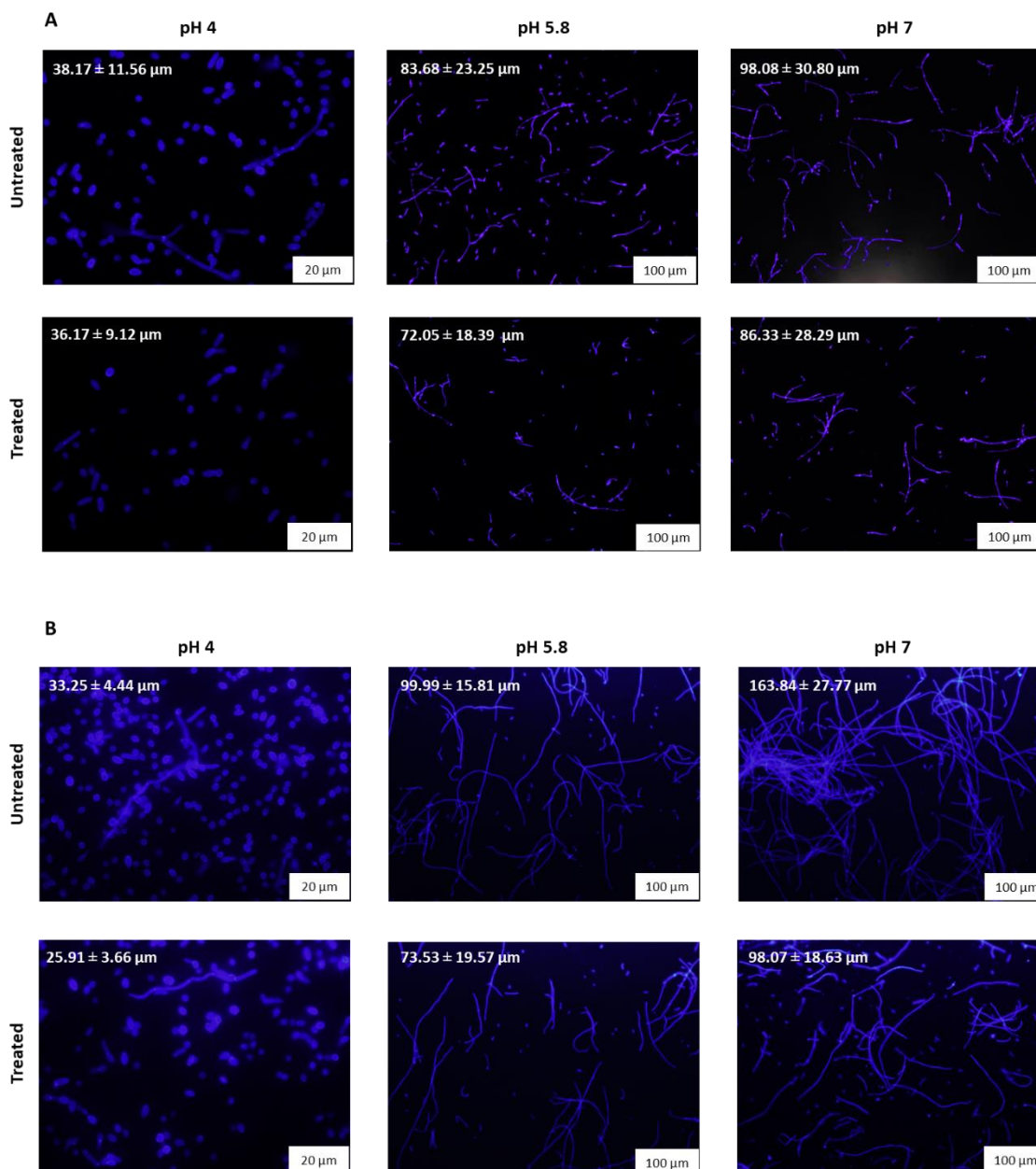
Figure 18. Anti-*RIM101* 2'OMe effect on *Candida albicans* cells length. Fluorescence microscopy images of *C. albicans* cells grown in RPMI (pH 4, 5.8 and 7) in the presence of 40 nM of anti-*RIMI101* 2'OMe, at 12 h **(A)** and 24 h **(B)**. Controls were prepared only with cells grown in RPMI (pH 4, 5.8 and 7) (without ASO).

At 24 h (figure 18A) the impact of anti-*RIM101* 2'OMe on filaments' length was the highest at pH 5.8 with a reduction from 100 µm to 74 µm and from 164 µm to 99 µm at pH 7. It is important to address that both ASOs possessed the highest effect on reduction of filaments length` at pH 5.8 and pH 7, curiously the conditions where *C. albicans* revealed to have major capacity to filament (Figure 13A).

3.3.5. Anti-*RAS1* 2'OMe and anti-*RIM101* 2'OMe performance on simulated body fluids

To infer about the stability and performance of anti-*RAS1* 2'OMe and anti-*RIM101* 2'OMe on simulated body fluids, *C. albicans* cells were grown on artificial urine (AU) at pH 4 and 5.8 and on artificial saliva (AS) at pH 7 in presence of 40 nM of each ASO or in presence of both ASOs.

3.3.5.1. Anti-*RAS1* 2'OMe and anti-*RIM101* 2'OMe individual performance

Figure 19A and 19B shows the effect of anti-*RAS1* 2'OMe and anti-*RIM101* 2'OMe individually on *C. albicans* cells filamentation when grown on simulated body fluids. The results revealed that the ASOs maintains its activity at all conditions.
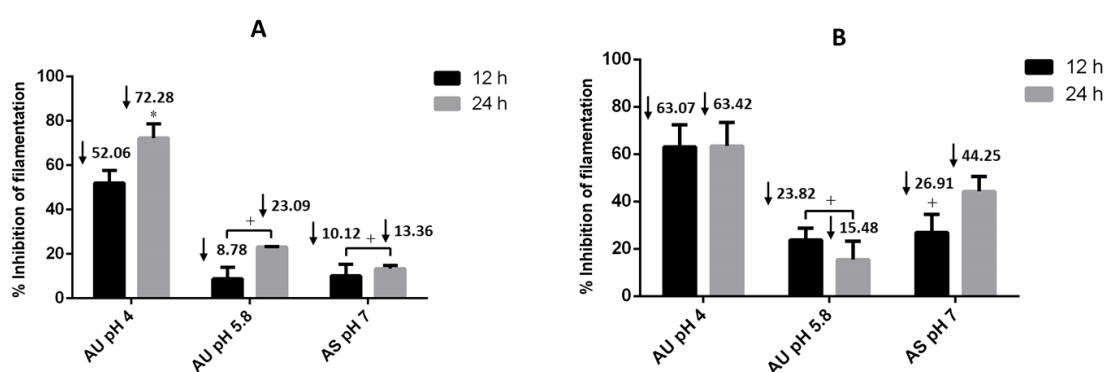
Figure 19. Individual performance of Anti-*RAS1* 2'OMe and Anti-*RIM101* 2'OMe on stimulated body fluids (A) Anti-*RAS1* 2'OMe and **(B)** anti-*RIM101* 2'OMe in AU (pH 4 and 5.8) and AS pH 7, treated with 40 nM of each ASO at 12 h and 24 h. Controls were prepared only with cells in AU (pH 4 and 5.8) and in AS (pH 7) (without ASO). Error bars represent standard derivation. *Significant differences between 12 h and 24 h for the same condition; ·Significant differences between AU pH 4 and other pH values for the same hour of incubation (P value <0.05).

The highest effect was observed on AU at pH 4, with values of reduction that increased from 52 % at 12 h for 72 % at 24 h (P value <0.05). In the case of AU at pH 5.8 and AS at pH 7, the percentage of *C. albicans'* filamentation inhibition was effectively lower, not reaching values higher than 23 % at 24 h on AU at pH 5.8 and 14 % on AS pH 7. The highest effect of anti-*RIM101* 2'OMe was on AU pH 4 with around 63 % of *C. albicans* filamentation reduction. On AS at pH 7, the inhibition of filamentation increased from 26 % at 12 h for 44 % at 24 h. In opposition, on AU at pH 5.8, the levels of reduction decreased from 24 % at 12 h to 16 % at 24h.

3.3.5.2.   Performance of a combination of Anti-*RAS1* 2'OMe and Anti-*RIM101* 2'OMe

As the main objective of this work is to contribute to the creation of a cocktail of ASOs able to totally inhibit *C. albicans'* filamentation the combined effect of anti-*RAS1* 2'OMe and anti-*RIM101* 2'OMe was evaluated. For that, a mixture of 40 nM of anti-*RAS1* 2'OMe and 40 nM of anti-*RIM101* 2'OMe was tested. The results revealed that the combination of the two ASOs potency the individual effect of each ASO in terms of the number of filaments reduction on AU at pH 5.8 and AS at pH 7 (Figure 20).
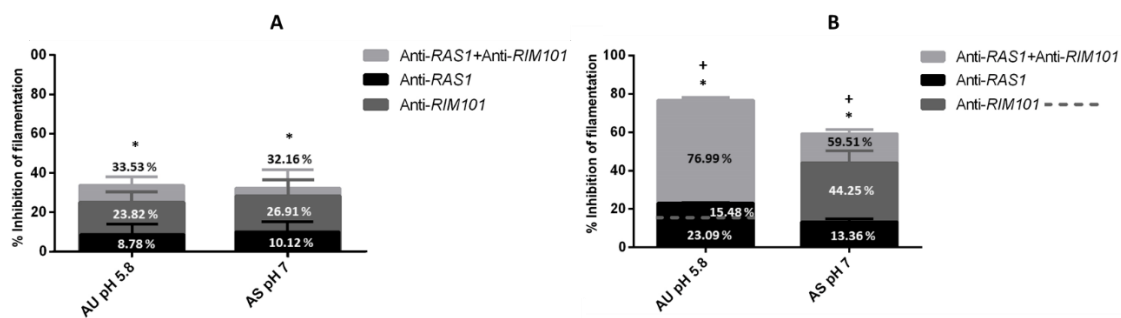
Figure 20. Combined performance of anti-*RAS1* 2'OMe and anti-*RIM101* 2'OMe on simulated body fluids. Individual performance of anti-*RAS1* 2'OMe and of anti-*RIM101* 2'OMe comparatively to the combined effect of anti-*RAS1* 2'OMe + anti-*RIM101* 2'OMe at 12 h **(A)** and 24 h **(B)** of *C. albicans* cells grown on artificial urine (AU) pH 5.8 and artificial saliva (AS) pH 7. Error bars represent standard derivation. *Significant differences between single anti-*RAS1* 2'OMe and combined effect for the same time of incubation. +Significant differences between single anti-*RIM101* 2'OMe and combined effect for the same time of incubation (P <0.05).

In the case of AU at pH 5.8 the percentage of inhibition increased from 34 % at 12 h to 77 % at 24 h (Figure 20B). On AS at pH 7, the combined effect of both ASOs also boosted the effect individual of each ASO resulting in a reduction of around 60 % after 24h (P <0.05). (Figure 20B). The singular condition where was not observed an additive effect was in the case of AS pH 7 after 24 h of *C. albicans* grown.

3.3.   Discussion

Despite an increasing number of successful applications of AST for the treatment of human chronic non-infectious diseases [97,104] and more recently, to manage infectious bacteria [111,112], this strategy was poorly exploited to control *C. albicans* virulence factors [135]. *Candida albicans* changes from commensal to pathogenic is primarily due to its morphological switch

between yeast and filamentous forms, a property that is central to penetrate human body tissues and escape the host´s immune system [51,142]. In the last decades, important technical advances have facilitated the investigation of the molecular biology of *C. albicans*' morphological transition as adaptation to different human environmental conditions [15,29,47]. Several works have demonstrated the importance of *RIM101* and *RAS1* genes as inducers of *C. albicans* filamentation [48,50,56,69]. The results obtained in the first part of this chapter reinforces the importance of *RIM101* and *RAS1* genes in *C. albicans* cells filamentation. The total *C. albicans* filamentation at pH 7 coupled with the highest levels of *RAS1* and *RIM101* expression (Figure 13) are an evidence of this fact. This makes *RIM101* and *RAS1* genes as ideal targets for applying AST to control virulence factors of *C. albicans*. Based on key hypothesis that if a pathogen`s genetic sequence of a specific gene is a determinant of virulence, as is the case of *RAS1* and *RIM101*, this work intended to project ASOs able to reduce the mRNA expression of *RAS1* and *RIM101* and, consequently, reduce its virulence phenotype (which, in this case, would be filaments' development). The second generation of nucleic mimics, specifically 2'OMe chemical modification, was the base for the anti-*RAS1* and anti-*RIM101* oligomers design [86].

It is assumed that ASOs must be projected with Tm around 39-42 °C and GC % of approximately 50-60 % in order to increase the binding affinity with target mRNA and stability in the human body [86,87]. Furthermore, several studies have shown that ASOs with size between 12 and 20 nts usually present a good hybridization performance [81,134]. Taking into account these features, the anti-*RAS1* 2'OMe and anti-*RIM101* 2'OMe sequences selected to be synthetized were the mUmGmG TTA AAC GGmG mAmU, with 42.0 °C of Tm, 42.9 % of GC, 14 nucleotides and mGmGmU GAC GTA GmCmAmU, with 44.9 °C of Tm, 53.8 % of GC, 13 nucleotides, for blocking *RAS1* and *RIM101* genes, respectively (Table 3). Three chemical modifications were added at each end of each sequence to increase the stability of the ASOs while maintaining the ability to recruit RNase H to degrade the mRNA [143]. Being a synthetic molecule, 2'OMe is not recognized by the RNase H, but a small DNA gap in the middle of the ASOs ensures the enzyme binding [74,87]. This way, the ASOs will act not only by directly blocking the protein synthesis but also by promoting the degradation of the target mRNA [74,96].

In order to determine the concentration of the ASOs to be used in the *in vitro* validation studies and in a future application *in vivo,* cytotoxicity tests were performed using a fibroblast cell line (3T3 cell line). Anti-*RAS1* 2'OMe and anti-*RIM101* 2'OMe did not demonstrated cytotoxicity since the relative fibroblasts cell viability is higher than 70 % comparatively to control (absence of ASOs)

(Figure 14)[141]. Therefore, it was decided to use 40 nM of ASO for the sub-sequent experimental tests.

As mentioned earlier, ASOs will be affecting *C. albicans* cellular functions through transcription genes expression attenuation and filamentous production. The effects of anti-*RAS1* 2'OMe and anti-*RIM101* 2'OMe on gene expression and on *C. albicans* filamentation were examined on acid and alkaline conditions over the time (Figures 15-18). The results revealed that both ASOs were able to block *RAS1* and *RIM101* genes expression, resulting in an inhibition of *C. albicans* filamentation in all conditions, although with different performances. In the case of anti-*RAS1* 2'OMe, it was observed a superior gene reduction at pH 7 at 12h of incubation (Figure 15A), reaching 95 % compared to pH 5.8 and 4 (39 % and 28 %, respectively). However, after 24 h (Figure 15B), the performance of the nanodrug was compromised at pH 7 (24 %) but not at pH 4 (54 %) and 5.8 (42 %). It is important to address that the highest level of *RAS1* expression (Figure 13B) was observed under this condition and could be the limitation to the performance of the anti-*RAS1* 2'OMe. Perhaps adding an extra dosage of oligomer every 12 h could be the solution to this problem.

Anti-*RIM101* 2'OMe showed to be more effective at 12 h in all conditions tested (figure 17A), with more than 50 % of reduction on gene expression levels. Over 24 h the anti-*RIM101* 2'OMe demonstrated to lose partially its capacity to block gene expression, at pH 4 and pH 5.8, but interestingly and, in contrast to anti-*RAS1* 2'OMe at pH 7, it was able to maintain its performance over the time with 73 % of reduction (Figure 17B). As expected, the blockage on *RAS1* and *RIM101* expression resulted in significant reduction on *C. albicans* filamentation and in filaments length´ (Figures 15C; 16; 17C and 18), however also with different performances. It is important to highlight that the dimorphic switching in *C. albicans* is dependent on a network of genes [36,56]. Thus, it was not expected a total reduction on *C. albicans* filamentation.

Interestingly, it can be noticed that anti-*RAS1* 2'OMe and anti-*RIM101* 2'OMe were able to maintain its activity on simulated human body fluids, reduction *C. albicans* filamentation (Figure 19). In fact, it was verified that on AU pH 4, values of 72 % of inhibition were achieved in the presence of anti-*RAS1* 2'OMe (Figure 19A) and 63 % (Figure 19B) in the presence of anti-*RIM101* 2'OMe. In AS pH 7, the anti-*RIM101* 2'OMe showed a greater capacity to reduce filamentous forms, reaching about 44 % after 24 h of treatment, contrarily to the results verified in the performance of anti-*RAS1* 2'OMe (14 %). Bearing in mind future medical applications, this result is very important,

since it confirms the ability of anti-*RAS1* 2'OMe and anti-*RIM101* 2'OMe as blocking agents in specific fluids, which are complex solutions with several components.

Lastly, as the main goal of this study is to contribute for developing an ASOs cocktail capable of totally reduce *C. albicans* filamentation, the combined effect of both ASOs was assessed (Figure 20). Importantly, it can be noticed an additive effect of both ASOs, resulting in an increase of around twice on the reduction of number of *C. albicans* cells' filamentation on almost all simulated human body fluids. Considering any possible future clinical medical applications of the ASOs cocktails in the control of local candidiasis (oral and urinary), these are important results once ASOs cocktail potency the individual effect of each ASO, maintaining its performance on human mimic body fluids.

Summarizing, the work developed under this chapter reinforces the hypothesis of AST as a promising alternative for the development of new alternative treatments for *Candida* infections.

4.   General Conclusions and Future Perspectives

4.1.   General Conclusion

A raise in antimicrobial resistance, the number of immunosuppressive patients and the restricted number of antifungal drugs have caused an increase of fungal infections, associated to *Candida* species. Furthermore, *C. albicans* continues to be the species responsible for the highest number of these infections, defined as candidiasis, with high rate of morbidity and mortality in health care and high associated costs. One of the most important *C. albicans* virulence factors is its ability to switch from yeast to filamentous forms (hyphae or/and pseusohyphae). Moreover, there are some speculations about the effect of the host's environmental conditions on this phenomenon. Thus, in the first part of the present work, it was aimed to deepen the knowledge about the behaviour of *C. albicans* in two simulated human body fluids (artificial saliva and urine) adjusted to different pH (pH 4, 5.8 and 7), in terms of growth and ability to develop filamentous forms. The results showed that *C. albicans* is able to grow and develop filaments in all conditions tested, but in different extensions. For example, *C. albicans* showed higher capacity for growing and cells with higher metabolic activity in AS although demonstrated less ability to develop filaments. Contrarily on AU, *C. albicans* demonstrated to have lower growth capacity associated with cells with lower metabolic activity, although the ability to form filaments was higher at pH 5.8 in comparison to other pH. This chapter reinforces the high plasticity and adaptability to different human body fluids with different compositions and different pH levels by *C. albicans* cells.

Thus, considering the high pathogenicity of *C. albicans* and the limitation of available antifungal agents, it is crucial to develop new approaches/therapies to the control of candidiasis on different human niches. AST can be a promising approach to control the complex network of genes adjacent to virulence factors, selectively blocking gene expression and consequently the corresponding protein function. The second part of this thesis confirms the involvement of *RAS1* and *RIM101* genes on regulation of *C. albicans* filamentation phenomenon. In this sense, projecting antisense oligomers targeting these two virulence determinants became the main goal of this thesis. The 2'OMe modification was the base to project the anti-*RAS1* 2'OMe and anti-*RIM101* 2'OMe that allow the mechanism of the mRNA degradation by RNase H. The ASOs were projected taking in consideration specific characteristics such as: the size of sequence (12-20 nucleotides), the melting temperature (39-42℃), the GC content (50-60 %), and the high specificity against *C. albicans* and low against *Homo sapiens*. It is important it to highlight that, anti-*RAS1* 2'OMe and

anti-*RIM101* 2'OMe were able to reduce the levels of expression of the correspondent genes targeted, as well as to control the filamentation capacity of *C. albicans*, although with different performances.

The levels of gene expression as well as the degree how *C. albicans* filament in each environmental condition influences the anti-*RAS1* 2'OMe and anti-*RIM101* 2'OMe performances. The present study also demonstrated that anti-*RAS1* 2'OMe and anti-*RIM101* 2'OMe maintains its activity on simulated body fluids (AU and AS), opening the door for future medical applications once fluid constituents do not seem to neutralize their function. Considering that, a virulence factor is regulated by a network of genes, the observed additive effect of the joint of the two ASOs highlights the need to build a cocktail of ASOs in order to fully control this and other virulence factors of *C. albicans*.

This work reinforces the promising applicability of AST in the control of virulence genes of *Candida* species and the consequent control of candidiasis.

4.2. Future Perspectives

The work described in this thesis provided an approach as useful to control *Candida* infections, leading to interesting new questions for further research. Some of these suggestions should be taken in consideration in order to deepen some of the results obtained and for developing further studies, namely:

- Studying the influence of the individual components (for example urea (AU) and mucin (AS)) of each simulated body fluid on the growth and filamentation of *C. albicans*;
- Transcriptomic analysis of *C. albicans* cells growing under different environmental human body conditions in order to identify new targets to apply AST;
- Projecting additional ASOs against other virulence determinants involved on *C. albicans* switch from yeast to filamentous' form in order to create an ASOs cocktail able to totally control this virulence factor;
- Study *in vivo* the potential effect of the *in vitro* validated ASOs.

5. References

1   McManus, B. A., & Coleman, D. C. (2014). Molecular epidemiology, phylogeny and evolution of Candida albicans. *Infection, Genetics and Evolution*, 21, 166-178.

2   Spampinato, C., & Leonardi, D. (2013). Candida infections, causes, targets, and resistance mechanisms: traditional and alternative antifungal agents. *BioMed research international*, 2013, 1-13.

3   Tellapragada, C., Eshwara, V. K., Johar, R., Shaw, T., Malik, N., Bhat, P. V., ... & Mukhopadhyay, C. (2014). Antifungal susceptibility patterns, in vitro production of virulence factors, and evaluation of diagnostic modalities for the speciation of pathogenic Candida from blood stream infections and vulvovaginal candidiasis. *Journal of pathogens*, 2014, 1-8.

4   Turner, S. A., & Butler, G. (2014). The Candida pathogenic species complex. Cold Spring Harbor perspectives in medicine, 4(9), 4-17.

5   Spivak, E. S., & Hanson, K. E. (2018). Candida auris: an emerging fungal pathogen. *Journal of clinical microbiology*, 56(2), 1-10.

6   Aydemir, Ö., Demiray, T., Köroğlu, M., Aydemir, Y., & Altındiş, M. (2017). Emerge of non-albicans Candida species; evaluation of Candida species and antifungal susceptibilities according to years. *Biomedical Research*, 28(6), 1-6.

7   Safavieh, M., Coarsey, C., Esiobu, N., Memic, A., Vyas, J. M., Shafiee, H., & Asghar, W. (2017). Advances in Candida detection platforms for clinical and point-of-care applications. *Critical reviews in biotechnology*, 37(4), 441-458.

8   Lohse, M. B., Gulati, M., Johnson, A. D., & Nobile, C. J. (2018). Development and regulation of single-and multi-species Candida albicans biofilms. *Nature Reviews Microbiology*, 16(1), 19-31.

9   Liu, S., Hou, Y., Chen, X., Gao, Y., Li, H., & Sun, S. (2014). Combination of fluconazole with non-antifungal agents: a promising approach to cope with resistant Candida albicans infections and insight into new antifungal agent discovery. *International journal of antimicrobial agents*, 43(5), 395-402.

10   Gow, N. A., & Yadav, B. (2017). Microbe Profile: Candida albicans: a shape-changing, opportunistic pathogenic fungus of humans. *Microbiology*, 163(8), 1145-1147.

11   Lim, C. Y., Rosli, R., Seow, H. F., & Chong, P. P. (2012). Candida and invasive candidiasis: back to basics. *European journal of clinical microbiology & infectious diseases*, 31(1), 21-31.

12   Álvares, C. A., Svidzinski, T. I. E., & Consolaro, M. E. L. (2007). Candidíase vulvovaginal: fatores predisponentes do hospedeiro e virulência das leveduras. *J. Bras. Patol. e Med. Lab.*, 43(5), 319-327.

13   Gulati, M., & Nobile, C. J. (2016). Candida albicans biofilms: development, regulation, and molecular mechanisms. *Microbes and infection*, 18(5), 310-321.

14   Richardson, J. P., & Moyes, D. L. (2015). Adaptive immune responses to Candida albicans infection. *Virulence*, 6(4), 327-337.

15   Glazier, V. E., & Krysan, D. J. (2018). Transcription factor network efficiency in the

regulation of Candida albicans biofilms: it is a small world. *Current genetics*, 64(4), 883-888.

16 Glazier, V. E., Murante, T., Murante, D., Koselny, K., Liu, Y., Kim, D., ... & Krysan, D. J. (2017). Genetic analysis of the Candida albicans biofilm transcription factor network using simple and complex haploinsufficiency. *PLoS genetics*, 13(8), 1-15.

17 Poulain, D. (2015). Candida albicans, plasticity and pathogenesis. *Critical reviews in microbiology*, 41(2), 208-217.

18 de Oliveira Santos, G. C., Vasconcelos, C. C., Lopes, A. J., de Sousa Cartágenes, M. D. S., do Nascimento, F. R., Ramos, R. M., ... & de Andrade Monteiro, C. (2018). Candida infections and therapeutic strategies: mechanisms of action for traditional and alternative agents. *Frontiers in microbiology*, 9, 1-23.

19 Singh, S., Fatima, Z., & Hameed, S. (2015). Predisposing factors endorsing Candida infections. *Le infezioni in medicina*, 23(3), 211-223.

20 Antinori, S., Milazzo, L., Sollima, S., Galli, M., & Corbellino, M. (2016). Candidemia and invasive candidiasis in adults: A narrative review. E*uropean journal of internal medicine*, 34, 21-28.

21 Motaung, T. E., Albertyn, J., Pohl, C. H., & Köhler, G. (2015). Candida albicans mutant construction and characterization of selected virulence determinants. *Journal of microbiological methods*, 115, 153-165.

22 Whibley, N., & Gaffen, S. L. (2015). Beyond Candida albicans: Mechanisms of immunity to non-albicans Candida species. *Cytokine*, 76(1), 42-52.

23 Chibana, H., Beckerman, J. L., & Magee, P. T. (2000). Fine-resolution physical mapping of genomic diversity in Candida albicans. *Genome research*, 10(12), 1865-1877.

24 Saghrouni, F. B. A. J., Ben Abdeljelil, J., Boukadida, J., & Ben Said, M. (2013). Molecular methods for strain typing of C andida albicans: a review. J*ournal of applied microbiology*, 114(6), 1559-1574.

25 Zhang, N., Magee, B. B., Magee, P. T., Holland, B. R., Rodrigues, E., Holmes, A. R., ... & Schmid, J. (2015). Selective advantages of a parasexual cycle for the yeast Candida albicans. *Genetics*, 200(4), 1117-1132.

26 Bennett, R. J. (2015). The parasexual lifestyle of Candida albicans. *Current opinion in microbiology*, 28, 10-17.

27 Motaung, T. E., Ells, R., Pohl, C. H., Albertyn, J., & Tsilo, T. J. (2017). Genome-wide functional analysis in Candida albicans. *Virulence*, 8(8), 1563-1579.

28 Berman, J. (2006). Morphogenesis and cell cycle progression in Candida albicans. *Current opinion in microbiology*, 9(6), 595-601.

29 Heitman, J. (2011). Microbial pathogens in the fungal kingdom. *Fungal biology reviews*, 25(1), 48-60.

30 McBride, A. E. (2017). Messenger RNA transport in the opportunistic fungal pathogen Candida albicans. *Current genetics*, 63(6), 989-995.

31 Kim, J., & Sudbery, P. (2011). Candida albicans, a major human fungal pathogen. *The Journal of Microbiology*, 49(2), 171-177.

32   Dadar, M., Tiwari, R., Karthik, K., Chakraborty, S., Shahali, Y., & Dhama, K. (2018). Candida albicans-Biology, molecular characterization, pathogenicity, and advances in diagnosis and control–An update. *Microbial pathogenesis*, 117, 128-138.

33   Sawant, B., & Khan, T. (2017). Recent advances in delivery of antifungal agents for therapeutic management of candidiasis. *Biomedicine & Pharmacotherapy*, 96, 1478-1490.

34   Mayer, F. L., Wilson, D., & Hube, B. (2013). Candida albicans pathogenicity mechanisms. *Virulence*, 4(2), 119-128.

35   Berman, J., & Sudbery, P. E. (2002). Candida albicans: a molecular revolution built on lessons from budding yeast. *Nature Reviews Genetics*, 3(12), 918-931.

36   Fox, E. P., Bui, C. K., Nett, J. E., Hartooni, N., Mui, M. C., Andes, D. R., ... & Johnson, A. D. (2015). An expanded regulatory network temporally controls C andida albicans biofilm formation. *Molecular microbiology*, 96(6), 1226-1239.

37   Chong, P. P., Chin, V. K., Wong, W. F., Madhavan, P., Yong, V. C., & Looi, C. Y. (2018). Transcriptomic and genomic approaches for unravelling Candida albicans biofilm formation and drug resistance—an update. *Genes*, 9(11), 1-19.

38   Tumbarello, M., Fiori, B., Trecarichi, E. M., Posteraro, P., Losito, A. R., De Luca, A., ... & Posteraro, B. (2012). Risk factors and outcomes of candidemia caused by biofilm-forming isolates in a tertiary care hospital. *PloS one*, 7(3), 1-9.

39   Kumamoto, C. A., & Vinces, M. D. (2005). Alternative Candida albicans lifestyles: growth on surfaces. *Annu. Rev. Microbiol.*, 59, 113-133.

40   Kojic, E. M., & Darouiche, R. O. (2004). Candida infections of medical devices. *Clinical microbiology reviews*, 17(2), 255-267.

41   Naglik, J., Albrecht, A., Bader, O., & Hube, B. (2004). Candida albicans proteinases and host/pathogen interactions. *Cellular microbiology*, 6(10), 915-926.

42   Benzaid, C., Belmadani, A., Djeribi, R., & Rouabhia, M. (2019). The effects of Mentha× piperita essential oil on C. albicans growth, transition, biofilm formation, and the expression of secreted aspartyl proteinases genes. *Antibiotics*, 8(1), 1-10.

43   Makanjuola, O., Bongomin, F., & Fayemiwo, S. A. (2018). An update on the roles of non-albicans Candida species in vulvovaginitis. *Journal of Fungi*, 4(4), 1-17.

44   Schaller, M., Borelli, C., Korting, H. C., & Hube, B. (2005). Hydrolytic enzymes as virulence factors of Candida albicans. *Mycoses*, 48(6), 365-377.

45   Ghannoum, M. A. (2000). Potential role of phospholipases in virulence and fungal pathogenesis. *Clinical microbiology reviews*, 13(1), 122-143.

46   Silva, S., Negri, M., Henriques, M., Oliveira, R., Williams, D. W., & Azeredo, J. (2012). Candida glabrata, Candida parapsilosis and Candida tropicalis: biology, epidemiology, pathogenicity and antifungal resistance. *FEMS microbiology reviews*, 36(2), 288-305.

47   Sudbery, P. E. (2011). Growth of Candida albicans hyphae. *Nature Reviews Microbiology*, 9(10), 737-748.

48   Du, H., & Huang, G. (2016). Environmental pH adaption and morphological transitions in Candida albicans. *Current genetics*, 62(2), 283-286.

49   Sharma, J., Rosiana, S., Razzaq, I., & Shapiro, R. S. (2019). Linking cellular morphogenesis

with antifungal treatment and susceptibility in Candida pathogens. *Journal of Fungi*, 5(1), 1-28.

50 Davis, D. (2003). Adaptation to environmental pH in Candida albicans and its relation to pathogenesis. *Current genetics*, 44(1), 1-7.

51 Huang, G. (2012). Regulation of phenotypic transitions in the fungal pathogen Candida albicans. *Virulence*, 3(3), 251-261.

52 Vylkova, S. (2017). Environmental pH modulation by pathogenic fungi as a strategy to conquer the host. *PLoS pathogens*, 13(2), 1-6.

53 Davis, D., Wilson, R. B., & Mitchell, A. P. (2000). RIM101-dependent and-independent pathways govern pH responses in Candida albicans. *Molecular and Cellular Biology*, 20(3), 971-978.

54 Bensen, E. S., Martin, S. J., Li, M., Berman, J., & Davis, D. A. (2004). Transcriptional profiling in Candida albicans reveals new adaptive responses to extracellular pH and functions for Rim101p. *Molecular microbiology*, 54(5), 1335-1351.

55 Román, E., Correia, I., Salazin, A., Fradin, C., Jouault, T., Poulain, D., ... & Pla, J. (2016). The Cek1-mediated MAP kinase pathway regulates exposure of α-1, 2 and β-1, 2-mannosides in the cell wall of Candida albicans modulating immune recognition. *Virulence*, 7(5), 558-577.

56 Basso, V., d'Enfert, C., Znaidi, S., & Bachellier-Bassi, S. (2018). From genes to networks: the regulatory circuitry controlling Candida albicans morphogenesis. *Fungal Physiology and Immunopathogenesis*, 61-99.

57 Hall, R. A., Cottier, F., & Mühlschlegel, F. A. (2009). Molecular networks in the fungal pathogen Candida albicans. *Advances in applied microbiology*, 67, 191-212.

58 Chen, J., Zhou, S., Wang, Q., Chen, X., Pan, T., & Liu, H. (2000). Crk1, a novel Cdc2-related protein kinase, is required for hyphal development and virulence in Candida albicans. *Molecular and Cellular Biology*, 20(23), 8696-8708.

59 Biswas, S., Van Dijck, P., & Datta, A. (2007). Environmental sensing and signal transduction pathways regulating morphopathogenic determinants of Candida albicans. *Microbiology and Molecular Biology Reviews*, 71(2), 348-376.

60 D'Souza, C. A., & Heitman, J. (2001). Conserved cAMP signaling cascades regulate fungal development and virulence. *FEMS microbiology reviews*, 25(3), 349-364.

61 Cao, C., Wu, M., Bing, J., Tao, L., Ding, X., Liu, X., & Huang, G. (2017). Global regulatory roles of the c AMP/PKA pathway revealed by phenotypic, transcriptomic and phosphoproteomic analyses in a null mutant of the PKA catalytic subunit in C andida albicans. *Molecular microbiology*, 105(1), 46-64.

62 Huang, G., Huang, Q., Wei, Y., Wang, Y., & Du, H. (2019). Multiple roles and diverse regulation of the Ras/cAMP/protein kinase A pathway in Candida albicans. *Molecular Microbiology*, 111(1), 6-16.

63 Hogan, D. A., & Sundstrom, P. (2009). The Ras/cAMP/PKA signaling pathway and virulence in Candida albicans. *Future microbiology*, 4(10), 1263-1270.

64 Inglis, D. O., & Sherlock, G. (2013). Ras signaling gets fine-tuned: regulation of multiple pathogenic traits of Candida albicans. *Eukaryotic cell*, 12(10), 1316-1325.

65   Villa, S., Hamideh, M., Weinstock, A., Qasim, M. N., Hazbun, T. R., Sellam, A., ... & Thangamani, S. (2020). Transcriptional control of hyphal morphogenesis in Candida albicans. *FEMS yeast research*, 20(1), 1-17.

66   Salvatori, O., Pathirana, R. U., Kay, J. G., & Edgerton, M. (2018). Candida albicans Ras1 inactivation increases resistance to phagosomal killing by human neutrophils. *Infection and immunity*, 86(12), 1-14.

67   Sonneborn, A., Bockmühl, D. P., Gerads, M., Kurpanek, K., Sanglard, D., & Ernst, J. F. (2000). Protein kinase A encoded by TPK2 regulates dimorphism of Candida albicans. *Molecular microbiology*, 35(2), 386-396.

68   Davis, D., Edwards, J. E., Mitchell, A. P., & Ibrahim, A. S. (2000). Candida albicans RIM101 pH response pathway is required for host-pathogen interactions. *Infection and immunity*, 68(10), 5953-5959.

69   Baek, Y. U., Martin, S. J., & Davis, D. A. (2006). Evidence for novel pH-dependent regulation of Candida albicans Rim101, a direct transcriptional repressor of the cell wall β-glycosidase Phr2. *Eukaryotic Cell*, 5(9), 1550-1559.

70   Garnaud, C., García-Oliver, E., Wang, Y., Maubon, D., Bailly, S., Despinasse, Q., ... & Cornet, M. (2018). The Rim pathway mediates antifungal tolerance in Candida albicans through newly identified Rim101 transcriptional targets, including Hsp90 and Ipt1. *Antimicrobial agents and chemotherapy*, 62(3), 1-14.

71   Hušeková, B., Elicharová, H., & Sychrová, H. (2016). Pathogenic Candida species differ in the ability to grow at limiting potassium concentrations. *Canadian journal of microbiology*, 62(5), 394-401.

72   Kurreck, J. (2003). Antisense technologies: improvement through novel chemical modifications. *European Journal of Biochemistry*, 270(8), 1628-1644.

73   Toth, P. P. (2011). Antisense therapy and emerging applications for the management of dyslipidemia. *Journal of clinical lipidology*, 5(6), 441-449.

74   Dias, N., & Stein, C. A. (2002). Antisense oligonucleotides: basic concepts and mechanisms. *Molecular cancer therapeutics*, 1(5), 347-355.

75   Thomas, T., & Ginsberg, H. (2010). Development of apolipoprotein B antisense molecules as a therapy for hyperlipidemia. *Current atherosclerosis reports*, 12(1), 58-65.

76   Taylor, M. F. (2001). Emerging antisense technologies for gene functionalization and drug discovery. *Drug discovery today*, 6, 97-101.

77   Warren, T. K., Whitehouse, C. A., Wells, J., Welch, L., Charleston, J. S., Heald, A., ... & Bavari, S. (2016). Delayed time-to-treatment of an antisense morpholino oligomer is effective against lethal marburg virus infection in cynomolgus macaques. PLoS neglected tropical diseases, 10(2), 1-19.

78   Kenney, S. P., & Meng, X. J. (2015). Therapeutic targets for the treatment of hepatitis E virus infection. *Expert opinion on therapeutic targets*, 19(9), 1245-1260.

79   Mansoor, M., & Melendez, A. J. (2008). Advances in antisense oligonucleotide development for target identification, validation, and as novel therapeutics. *Gene regulation and systems biology*, 2, 275–295

80   Stebbins, C. C., Petrillo, M., & Stevenson, L. F. (2019). Immunogenicity for antisense

oligonucleotides: a risk-based assessment. *Bioanalysis* 11, 1913–1916

81 Batista-Duharte, A., Sendra, L., Herrero, M. J., Téllez-Martínez, D., Carlos, I. Z., & Aliño, S. F. (2020). Progress in the use of antisense oligonucleotides for vaccine improvement. *Biomolecules*, 10(2), 316.

82 Bennett, C. F., & Swayze, E. E. (2010). RNA targeting therapeutics: molecular mechanisms of antisense oligonucleotides as a therapeutic platform. *Annual review of pharmacology and toxicology*, 50, 259-293.

83 Bennett, C. F. (2019). Therapeutic antisense oligonucleotides are coming of age. *Annual review of medicine*, 70, 307-321.

84 Hendling, M., & Barišić, I. (2019). In-silico design of DNA oligonucleotides: challenges and approaches. *Computational and structural biotechnology journal*, 17, 1056-1065.

85 Evers, M. M., Toonen, L. J., & van Roon-Mom, W. M. (2015). Antisense oligonucleotides in therapy for neurodegenerative disorders. *Advanced drug delivery reviews*, 87, 90-103.

86 Chan, J. H., Lim, S., & Wong, W. F. (2006). Antisense oligonucleotides: from design to therapeutic application. *Clinical and experimental pharmacology and physiology*, 33(5-6), 533-540.

87 DeVos, S. L., & Miller, T. M. (2013). Antisense oligonucleotides: treating neurodegeneration at the level of RNA. *Neurotherapeutics*, 10(3), 486-497.

88 Monia, B. P., Johnston, J. F., Ecker, D. J., Zounes, M. A., Lima, W. F., & Freier, S. M. (1992). Selective inhibition of mutant Ha-ras mRNA expression by antisense oligonucleotides. *Journal of Biological Chemistry*, 267(28), 19954-19962.

89 Crooke, S. T. (2004). Antisense strategies. *Current molecular medicine*, 4(5), 465-487.

90 Peacey, E., Rodriguez, L., Liu, Y., & Wolfe, M. S. (2012). Targeting a pre-mRNA structure with bipartite antisense molecules modulates tau alternative splicing. *Nucleic acids research*, 40(19), 9836-9849.

91 Krol, J., Loedige, I., & Filipowicz, W. (2010). The widespread regulation of microRNA biogenesis, function and decay. *Nature Reviews Genetics*, 11(9), 597-610.

92 Huntzinger, E. and Izaurralde, E. (2011) Gene silencing by microRNAs: Contributions of translational repression and mRNA decay. *Nat. Rev. Genet.* 12, 99–110.

93 Lanford, R. E., Hildebrandt-Eriksen, E. S., Petri, A., Persson, R., Lindow, M., Munk, M. E., ... & Ørum, H. (2010). Therapeutic silencing of microRNA-122 in primates with chronic hepatitis C virus infection. *Science*, 327(5962), 198-201.

94 Janssen, H. L., Reesink, H. W., Lawitz, E. J., Zeuzem, S., Rodriguez-Torres, M., Patel, K., ... & Hodges, M. R. (2013). Treatment of HCV infection by targeting microRNA. *New England Journal of Medicine*, 368(18), 1685-1694.

95 Crooke, S. T., Witztum, J. L., Bennett, C. F., & Baker, B. F. (2018). RNA-targeted therapeutics. *Cell metabolism*, 27(4), 714-739.

96 Hegarty, J. P., & Stewart, D. B. (2018). Advances in therapeutic bacterial antisense biotechnology. *Applied microbiology and biotechnology*, 102(3), 1055-1065.

97 Miller, K.M.S. & T.M. (2017) Antisense oligonucleotides: Translation from mouse models to human neurodegenerative diseases Kathleen. *Physiol. Behav.* 176, 139–148.

98   Khvorova, A., & Watts, J. K. (2017). The chemical evolution of oligonucleotide therapies of clinical utility. *Nature biotechnology*, 35(3), 238-248.

99   Sardone, V., Zhou, H., Muntoni, F., Ferlini, A., & Falzarano, M. S. (2017). Antisense oligonucleotide-based therapy for neuromuscular disease. *Molecules*, 22(4), 1-24.

100   Frazier, K. S. (2015). Antisense oligonucleotide therapies: the promise and the challenges from a toxicologic pathologist's perspective. *Toxicologic pathology*, 43(1), 78-89.

101   Swayze, E. E., Siwkowski, A. M., Wancewicz, E. V., Migawa, M. T., Wyrzykiewicz, T. K., Hung, G., ... & Bennett, A. C. F. (2007). Antisense oligonucleotides containing locked nucleic acid improve potency but cause significant hepatotoxicity in animals. *Nucleic acids research*, 35(2), 687-700.

102   GrÜnweiler, A., & Hartmann, R. K. (2007). Locked nucleic acid oligonucleotides. *BioDrugs*, 21(4), 235-243.

103   Dassie, J. P., & Giangrande, P. H. (2013). Current progress on aptamer-targeted oligonucleotide therapeutics. *Therapeutic delivery*, 4(12), 1527-1546.

104   Spraggon, L., & Cartegni, L. (2013). Antisense modulation of RNA processing as a therapeutic approach in cancer therapy. *Drug Discovery Today: Therapeutic Strategies*, 10(3), e139-e148.

105   Salameh, A., Lee, A. K., Cardó-Vila, M., Nunes, D. N., Efstathiou, E., Staquicini, F. I., ... & Arap, W. (2015). PRUNE2 is a human prostate cancer suppressor regulated by the intronic long noncoding RNA PCA3. *Proceedings of the National Academy of Sciences*, 112(27), 8403-8408.

106   Velez, M. V. L., Verhaegh, G. W., Smit, F., Sedelaar, J. M., & Schalken, J. A. (2019). Suppression of prostate tumor cell survival by antisense oligonucleotide-mediated inhibition of AR-V7 mRNA synthesis. *Oncogene*, 38(19), 3696-3709.

107   Chuan, L., Xiaohou, W., Chunli, L., Zili, H., Zhikang, Y., Yunfeng, H., ... & Yanjun, L. (2010). Antisense oligonucleotide targeting Livin induces apoptosis of human bladder cancer cell via a mechanism involving caspase 3. *Journal of experimental & clinical cancer research*, 29(1), 1-8.

108   Hong, J. H., Lee, E., Hong, J., Shin, Y. J., & Ahn, H. (2002). Antisense Bcl2 oligonucleotide in cisplatin-resistant bladder cancer cell lines. *BJU international*, 90(1), 113-117.

109   Mogilevsky, M., Shimshon, O., Kumar, S., Mogilevsky, A., Keshet, E., Yavin, E., ... & Karni, R. (2018). Modulation of MKNK2 alternative splicing by splice-switching oligonucleotides as a novel approach for glioblastoma treatment. *Nucleic acids research*, 46(21), 11396-11404.

110   Petrescu, G. E., Sabo, A. A., Torsin, L. I., Calin, G. A., & Dragomir, M. P. (2019). MicroRNA based theranostics for brain cancer: basic principles. *Journal of experimental & clinical cancer research*, 38(1), 1-21.

111   Montagner, G., Bezzerri, V., Cabrini, G., Fabbri, E., Borgatti, M., Lampronti, I., ... & Gambari, R. (2017). An antisense peptide nucleic acid against Pseudomonas aeruginosa inhibiting bacterial-induced inflammatory responses in the cystic fibrosis IB3-1 cellular model system. *International journal of biological macromolecules*, 99, 492-498.

112   Ghosal, A., & Nielsen, P. E. (2012). Potent antibacterial antisense peptide–peptide nucleic

acid conjugates against Pseudomonas aeruginosa. *Nucleic acid therapeutics*, 22(5), 323-334.

113 Araújo, D., Azevedo, N. M., Barbosa, A., Almeida, C., Rodrigues, M. E., Henriques, M., & Silva, S. (2019). Application of 2′-OMethylRNA′ Antisense Oligomer to Control Candida albicans EFG1 Virulence Determinant. *Molecular Therapy-Nucleic Acids*, 18, 508-517.

114 Singh, D. K., Tóth, R., & Gácser, A. (2020). Mechanisms of pathogenic Candida species to evade the host complement attack. *Frontiers in cellular and infection microbiology*, 10, 94.

115 Pellon, A., Sadeghi Nasab, S. D., & Moyes, D. L. (2020). New insights in Candida albicans innate immunity at the mucosa: toxins, epithelium, metabolism, and beyond. *Frontiers in cellular and infection microbiology*, 10, 81.

116 Pereira, L., Silva, S., Ribeiro, B., Henriques, M., & Azeredo, J. (2015). Influence of glucose concentration on the structure and quantity of biofilms formed by Candida parapsilosis. *FEMS yeast research*, 15(5), 1-7.

117 Vylkova, S., Carman, A. J., Danhof, H. A., Collette, J. R., Zhou, H., & Lorenz, M. C. (2011). The fungal pathogen Candida albicans autoinduces hyphal morphogenesis by raising extracellular pH. *MBio*, 2(3), 1-12.

118 Humphrey, S. P., & Williamson, R. T. (2001). A review of saliva: normal composition, flow, and function. *The Journal of prosthetic dentistry*, 85(2), 162-169.

119 Dewar, S., Reed, L. C., & Koerner, R. J. (2014). Emerging clinical role of pivmecillinam in the treatment of urinary tract infection in the context of multidrug-resistant bacteria. *Journal of Antimicrobial Chemotherapy*, 69(2), 303-308.

120 Silva, S., Pires, P., Monteiro, D. R., Negri, M., Gorup, L. F., Camargo, E. R., ... & Azeredo, J. (2013). The effect of silver nanoparticles and nystatin on mixed biofilms of Candida glabrata and Candida albicans on acrylic. *Medical mycology*, 51(2), 178-184.

121 Silva, S., Negri, M., Henriques, M., Oliveira, R., Williams, D., & Azeredo, J. (2010). Silicone colonization by non-Candida albicans Candida species in the presence of urine. *Journal of medical microbiology*, 59(7), 747-754.

122 Williams, D. W., Wilson, M. J., Lewis, M. A., & Potts, A. J. (1995). Identification of Candida species by PCR and restriction fragment length polymorphism analysis of intergenic spacer regions of ribosomal DNA. *Journal of Clinical Microbiology*, 33(9), 2476-2479.

123 Silva, S., Henriques, M., Oliveira, R., Williams, D., & Azeredo, J. (2010). In vitro biofilm activity of non-Candida albicans Candida species. *Current microbiology*, 61(6), 534-540.

124 Tronchin, G., Pihet, M., Lopes-Bezerra, L. M., & Bouchara, J. P. (2008). Adherence mechanisms in human pathogenic fungi. *Sabouraudia*, 46(8), 749-772.

125 Moffa, E. B., Izumida, F. E., Mussi, M. C. M., Siqueira, W. L., Jorge, J. H., & Giampaolo, E. T. (2016). Interaction between XTT assay and candida albicans or streptococcus mutans viability. *Journal of International Oral Health*, 8(1), 12.

126 Kuhn, D. M., Balkis, M., Chandra, J., Mukherjee, P. K., & Ghannoum, M. A. (2003). Uses and limitations of the XTT assay in studies of Candida growth and metabolism. *Journal of clinical microbiology*, 41(1), 506-508.

127 Honraet, K., Goetghebeur, E., & Nelis, H. J. (2005). Comparison of three assays for the quantification of Candida biomass in suspension and CDC reactor grown biofilms. *Journal*

of Microbiological Methods, 63(3), 287-295.

128   Lazarin, A. A., Machado, A. L., Zamperini, C. A., Wady, A. F., Spolidorio, D. M. P., & Vergani, C. E. (2013). Effect of experimental photopolymerized coatings on the hydrophobicity of a denture base acrylic resin and on Candida albicans adhesion. *Archives of oral biology*, 58(1), 1-9.

129   Valentijn-Benz, M., Nazmi, K., Brand, H. S., van't Hof, W., & Veerman, E. C. (2015). Growth of Candida albicans in human saliva is supported by low-molecular-mass compounds. *FEMS yeast research*, 15(8), 1-8.

130   Salvatori, O., Puri, S., Tati, S., & Edgerton, M. (2016). Innate immunity and saliva in Candida albicans–mediated oral diseases. *Journal of dental research*, 95(4), 365-371.

131   Uppuluri, P., Dinakaran, H., Thomas, D. P., Chaturvedi, A. K., & Lopez-Ribot, J. L. (2009). Characteristics of Candida albicans biofilms grown in a synthetic urine medium. *Journal of clinical microbiology*, 47(12), 4078-4083.

132   Araújo, D., Henriques, M., & Silva, S. (2017). Portrait of Candida species biofilm regulatory network genes. *Trends in microbiology*, 25(1), 62-75.

133   Sully, E. K., & Geller, B. L. (2016). Antisense antimicrobial therapeutics. *Current opinion in microbiology*, 33, 47-55.

134   Disney, M. D., Haidaris, C. G., & Turner, D. H. (2003). Uptake and antifungal activity of oligonucleotides in Candida albicans. *Proceedings of the National Academy of Sciences*, 100(4), 1530-1534.

135   Odeh, F., Nsairat, H., Alshaer, W., Ismail, M. A., Esawi, E., Qaqish, B., ... & Ismail, S. I. (2020). Aptamers chemistry: Chemical modifications and conjugation strategies. *Molecules*, 25(1), 1-51.

136   Medrano, G., Guan, P., Barlow-Anacker, A. J., & Gosain, A. (2017). Comprehensive selection of reference genes for quantitative RT-PCR analysis of murine extramedullary hematopoiesis during development. *PLoS One*, 12(7), 1-15.

137   Pfaffl, M. W. (2001). A new mathematical model for relative quantification in real-time RT–PCR. *Nucleic acids research*, 29(9), e45-e45.

138   Stein, C. A. (2001). The experimental use of antisense oligonucleotides: a guide for the perplexed. *The Journal of clinical investigation*, 108(5), 641-644.

139   Stepanenko, A. A., & Dmitrenko, V. V. (2015). Pitfalls of the MTT assay: Direct and off-target effects of inhibitors can result in over/underestimation of cell viability. *Gene*, 574(2), 193-203.

140   Chen, J., Cheng, G. H., Chen, L. P., Pang, T. Y., & Wang, X. L. (2013). Prediction of chemotherapeutic response in unresectable non-small-cell lung cancer (NSCLC) patients by 3-(4, 5-dimethylthiazol-2-yl)-5-(3-carboxymethoxyphenyl)-2-(4-sulfophenyl)-2H-tetrazolium (MTS) assay. *Asian Pacific Journal of Cancer Prevention*, 14(5), 3057-3062.

141   (CSA), C.S.A. (2009) ISO 10993-5 in vitro cytotoxicity. *Int. Organ.* 2007, 1–11

142   Uwamahoro, N., Verma-Gaur, J., Shen, H. H., Qu, Y., Lewis, R., Lu, J., ... & Traven, A. (2014). The pathogen Candida albicans hijacks pyroptosis for escape from macrophages. *MBio*, 5(2), 1-11.

143   Powell, T. (1972). A mathematical model for calcium homeostasis. *The Bulletin of mathematical biophysics*, 34(4), 483-502.

6. Annex

Annex I

Growth rate

Figure AI.1 shows the results obtained for the specific growth rate for all conditions tested through linear regression.
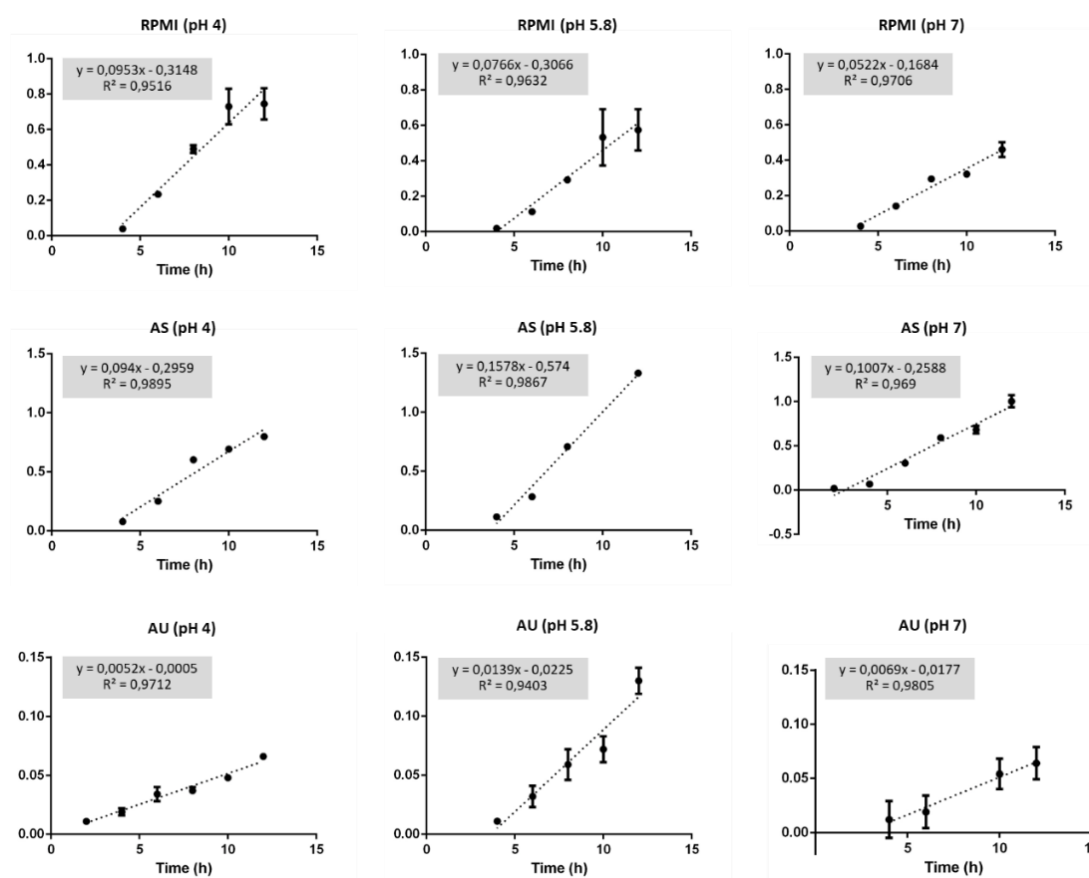

Figure AI.1 Specific growth rate. Results of linear regression of the exponential growth phase of *C. albicans* SC5314 in RPMI (pH 4, 5.8 and 7), AS (pH 4, 5.8 and 7) and AU (pH 4, 5.8 and 7). Error bars represent standard deviation.

pH monitoring

pH of each fluid at beginning (T0) and after 24 h of incubation with *C. albicans* (Figure AI.2). In fact, for both fluids tested was possible observe that on AS after 24 h of incubation the pH variations were significant at pH 4 (6.00) and 5.8 (7.27) compared to other conditions [AS pH 7 (6.60); AU pH 4 (3.31); AU pH 5.8 (5.23) and AU pH 7 (7.26)].
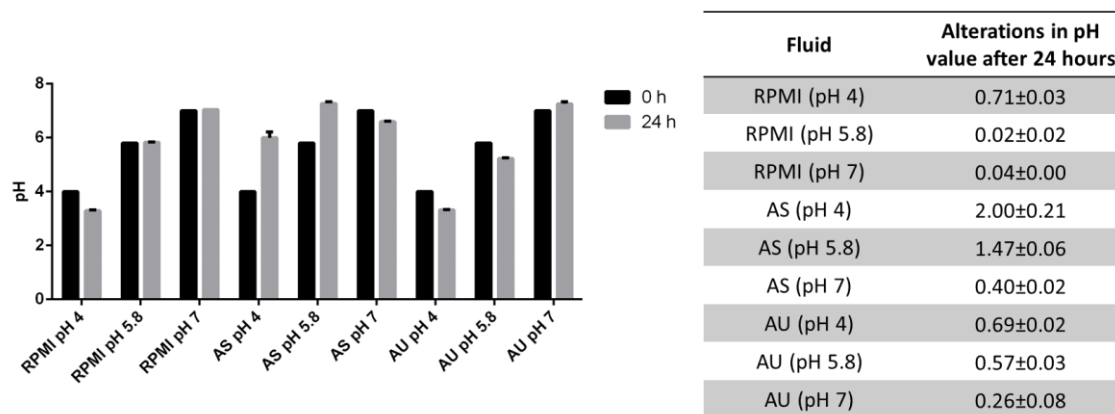
Figure AI.2 Values of pH for each fluid tested. pH values at the beginning and after 24 h incubation with *C. albicans* SC5314 in RPMI (pH 4, 5.8 and 7), AS (pH 4, 5.8 and 7) and AU (pH 4, 5.8 and 7).

Metabolic activity

The cells metabolic activity of *C. albicans* was determined through the XTT reduction assay (Figure AI.3).
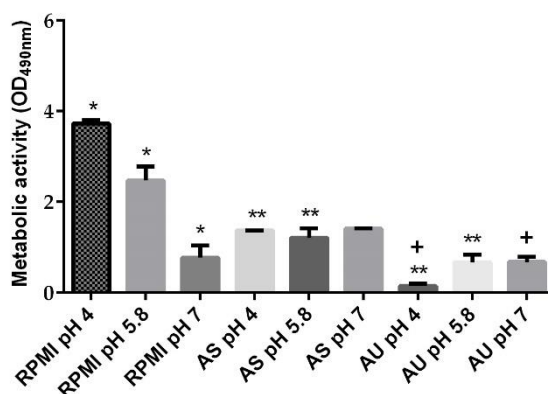

Figure AI.3 *Candida albicans* metabolic activity determination on simulated human body fluids. Metabolic activity determination by XTT reduction (Abs 490 nm) obtained for planktonic growth of *C. albicans* SC5314 in RPMI (pH 4, 5.8 and 7), AS (pH 4, 5.8 and 7) and AU (pH 4, 5.8 and 7), at 24 h. Error bars represent standard deviation. *Significant differences between the same condition and different pH value; **Significant differences between RPMI and same fluid pH value; +Significant differences between different fluid and same pH value (P value <0.05).

The results showed that *C. albicans* evidence higher metabolic activity in RPMI pH 4 and pH 5.8 when compared with AS and AU, with statistically different (P value <0.05). In fact, the

metabolic activity in RPMI decreases as the pH becomes more alkaline (P value <0.05). In AS and AU fluids, there are no significant differences in the different pH values, although in AU pH 4 there is a slight decrease of cell metabolic activity.

Annex II

AOS´s design

In table AII.1, it is possible to observe potential sequences to be used for the design of the nanodrugs capable of hybridizing with selected genes in order to inhibit its mRNA and block the function of its proteins.

Table AII.1 Different sequences for antisense oligomers design. Sequences, length, melting temperature (Tm) and GC content (% GC).

Gene	Systematic name	Sequences	Length	Tm (°C)	% GC
RAS1	C2_10210C_A (orf19.1760)	ATCCGCTTTAACCAT	15	44	40
		ATCCGCTTTAACCA	**14**	**43**	**43**
		GACCCAACTATTGA	14	39	43
		AGAAGAATATCTGGC	15	40	40
RIM101	C1_14340C_A (orf19.7247)	TACCGGTGCAAGT	13	45	54
		AGTCCCCATTCCTC	14	45	57
		ATGCTACGTCACC	**13**	**42**	**54**

Inhibition of gene expression

Figures AII.1 and AII.2 show the effects of anti-*RAS1* 2'OMe and anti-*RIM101* 2'OMe on inhibiting gene expression, respectively.
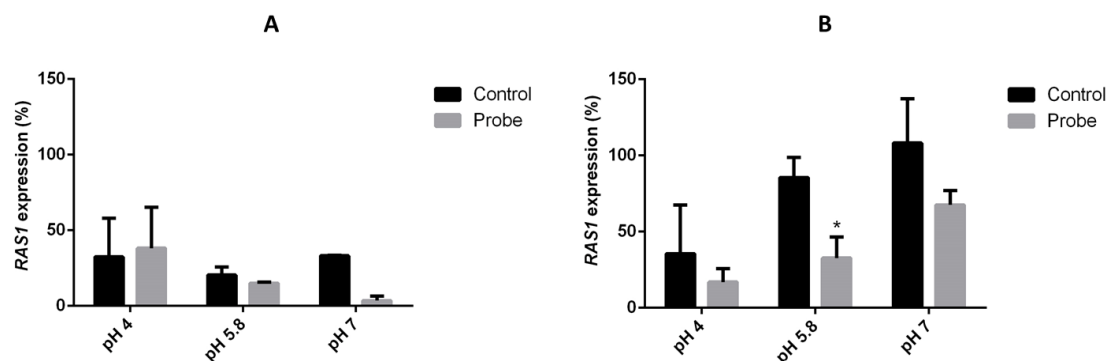

Figure AII.1 Anti-*RAS1* 2'OMe effects on *Candida albicans*. Levels of *RAS1* gene expression obtained by the *ΔCt* method, at 12 h **(A)** and 24 h **(B)** after treatment with 40 nM of anti-*RAS1* 2'OMe in RPMI under different pH values (pH 4, 5.8 and 7). Controls (untreated) were prepared only with cells on RPMI (pH 4, 5.8 and 7) (without ASO). Error bars represent standard derivation. *Significantly differences between controls and cells treated with 40 nM of anti-*RAS1* 2'OMe (P value <0.05).
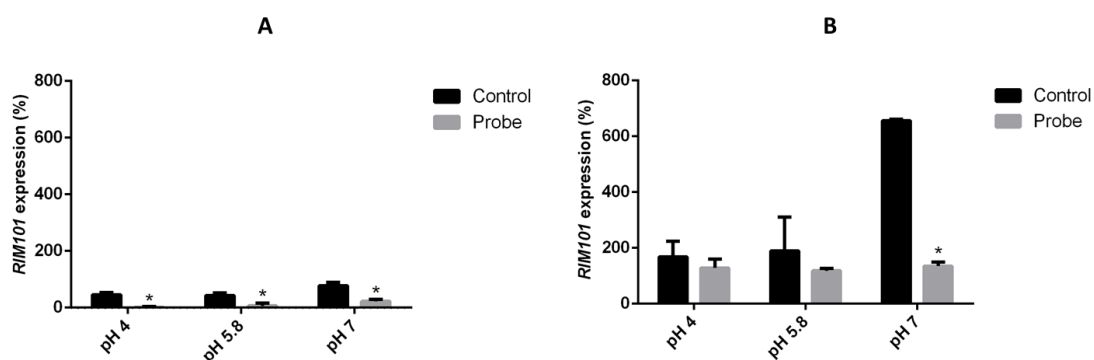

Figure AII.2 Anti-*RIM101* 2'OMe effects on *Candida albicans*. Levels of *RIM101* gene expression obtained by the *ΔCt* method, at 12 h **(A)** and 24 h **(B)** after treatment with 40 nM of anti-*RIM101* 2'OMe in RPMI under different pH values (pH 4, 5.8 and 7). Controls (untreated) were prepared only with cells on RPMI (pH 4, 5.8 and 7) (without ASO). Error bars represent standard derivation. *Significantly differences between controls and cells treated with 40 nM of anti-*RAS1* 2'OMe (P value <0.05).